POLITECNICO DI TORINO

Master's Degree in Aerospace Engineering

Master's Degree Thesis

An electric motorized dispenser for In-Orbit Servicing

Supervisors

Prof.ssa Manuela BATTIPEDE

Co-supervisors

Ing. Luigi MASCOLO

Dott. Francesco FRAGNITO

Candidate

Sabato IULIANO

July 2021

POLITECNICO DI TORINO

Master's Degree in Aerospace Engineering

Master's Degree Thesis

An electric motorized dispenser for In-Orbit Servicing

Supervisors

Prof.ssa Manuela BATTIPEDE

Co-supervisors

Ing. Luigi MASCOLO

Dott. Francesco FRAGNITO

Candidate

Sabato IULIANO

July 2021

A mio padre Raffaele

Summary

The thesis work presented below was born in the context of a collaboration carried out with SAB Launch Services srl of Benevento aimed at identifying an engineering solution based on motorizing the hexagonal module of the Small Spacecraft Mission Service (SSMS). Given the nature of the company itself, the ultimate aim of this work will be to provide a starting point for the development of a system, here renamed IOSHEXA, essentially oriented to In-Orbit Servicing. At the request of SAB Launch Services itself, the analysis turned to an exclusively electric motorization, this choice therefore allowed the carrying out of a parametric mission analysis that would allow the identification of an ideal solution. The results obtained from the mission analysis for electric propulsion were then compared with the data of electric motors collected during these months of work in the company in order to identify, through a trade-off, the best real solution currently available among those considered.

Table of Contents

List of Figures IX

List of Tables XI

Symbols XIII

Acronyms XVI

1 Introduction 1
- 1.1 IOSHEXA concept 2
  - 1.1.1 Release and positioning of small-sat 3
  - 1.1.2 Debris Removal 4
  - 1.1.3 IOSHEXA IOD mission 8

2 Fundamentals of Astrodynamics 11
- 2.1 Keplerian Orbits 11
  - 2.1.1 Newton's Laws 11
  - 2.1.2 Two-body problem 12
  - 2.1.3 Two-body equation of motion 13
  - 2.1.4 Constants of the motion 15
  - 2.1.5 The trajectory equation 15
  - 2.1.6 Classical Orbital Elements 18
- 2.2 Orbital Maneuvers 20
  - 2.2.1 Adjustment of Periapsis and Apoapsis Height 20
  - 2.2.2 The Hohmann Transfer 21
  - 2.2.3 General Coplanar Transfer 22
  - 2.2.4 Orbit Rendezvous 25
  - 2.2.5 Orbit Plane Changes 26

3 Electric Propulsion 29
- 3.1 Generalities of space propulsion 30

3.1.1 Rocket Equation 32
3.1.2 Velocity Losses 33
3.2 Electric propulsion maneuvers 34
3.2.1 Coplanar Circle-to-Circle Transfer 38
3.2.2 Inclination-Change Maneuver 39
3.2.3 Transfer Between Inclined Circular Orbits 40
3.2.4 Walking 40
3.3 Electric Thrusters 41
3.3.1 Hall Effect Thrusters 44
3.3.2 Enhanced Magnetic Plasma Thrusters 46
3.3.3 Microwave Electrothermal thrusters 47

4 Mission Analysis for electric propulsion 51
4.1 Preliminary Analysis 55
4.1.1 Mission: Δv 58
4.1.2 Strategy: T 61
4.1.3 Technological Level: β 64
4.1.4 Time: Δt 64
4.2 Mission analysis IOSHEXA 65
4.2.1 Analysis of results 78
4.2.2 Trade-Off Propulsion Systems 79

5 Conclusions 83

A ΔV Preliminary evaluation 85

B Thrusting time 89

C Mission analysis for electric propulsion 91
C.1 Mission-Strategy-Technological Level 91
C.2 Mission-Time-Technological Level 93

Bibliography 97

List of Figures

1.1 Small Spacecraft Mission Services (*SSMS*) 2
1.2 ESA built-solar cells retrieved from the Hubble Space Telescope in 2002 4
1.3 Business as Usual 6
1.4 Implementation of Space Debris Mitigation 6
1.5 Future debris density at poles with and without active debris removal 7

2.1 Representation of the generic two-body problem in an Inertial Reference Frame 12
2.2 Two-body problem in a polar coordinate system 14
2.3 Conic sections 16
2.4 Elliptical Orbit 17
2.5 Classical Orbital Elements [6] 18
2.6 Apoapsis Lowering [7] 20
2.7 Periapsis Raising [7] 20
2.8 Hohmann Transfer [7] 21
2.9 Coplanar Transfer [7] 23
2.10 p versus e [8] 24
2.11 Rendezvous Example [7] 25
2.12 Simple Plane Change [7] 26

3.1 Forces affecting the vehicle's motion [7] 33
3.2 Thrust and its components ($N \equiv R$) [7] 35
3.3 Coplanar Circle-to-Circle Transfer [7] 38
3.4 Inclination Change [10] 39
3.5 General shape of the Walking maneuver. $\delta\theta$ is the advance angle relative to a hypothetical satellite remaining in the original orbit and left undisturbed. [11] 40
3.6 Δv for the Walking maneuver [11]. 41
3.7 Scheme for application of first principle to electric propulsion (subscript 0 means input, subscript e means exit). 42

3.8 Schematic of an Hall Effect Thruster [12] 44
3.9 Hall Effect in an HET [12] 45
3.10 Enhanced Magnetic Plasma Thruster [13] 47
3.11 Microwave Electrothermal Thruster Schematic 48

4.1 c_{opt} example [8] 53
4.2 Reference Orbit of the IOD mission 58
4.3 ExoMG - micro in operation [17] 62
4.4 REGULUS [18] 63
4.5 AQUAMET [19] 63
4.6 Optimal I_{sp} for case 1a 66
4.7 Optimal I_{sp} for case 2a 67
4.8 Optimal I_{sp} for case 3a 68
4.9 Optimal I_{sp} for case 4a 69
4.10 Optimal I_{sp} for case 1b 70
4.11 Optimal I_{sp} for case 2b 71
4.12 Optimal I_{sp} for case 3b 72
4.13 Optimal I_{sp} for case 4b 73
4.14 Optimal I_{sp} for case 1c 74
4.15 Optimal I_{sp} for case 2c 75
4.16 Optimal I_{sp} for case 1d 76
4.17 Optimal I_{sp} for case 2d 77
4.18 Excel-table: trade-off results 80
4.19 Radar graphic - Propulsion Trade-off 81

List of Tables

1.1 Contributions by macro object to the MASTER-2005 model reference population discriminated by size regimes, orbital regions and sources in LEO [2] . . . 5
1.2 Orbits specifications in the IOD mission . . . 8

2.1 Geometrical properties common to all conic sections . . . 16
2.2 Relating E_g to the geometry of an orbit [5] . . . 18
2.3 Classical Orbital Elements . . . 19

3.1 Hall Effect - Ion Thrusters Comparison . . . 46

4.1 Integration and Test Operations . . . 56
4.2 Launch Operations . . . 56
4.3 Technological Demonstrator Operations . . . 57
4.4 End of Life . . . 58
4.5 Δv resume . . . 61
4.6 Thrusters specific [20],[21] (* esteem) . . . 64
4.7 Input for case 1a . . . 66
4.8 Output for case 1a . . . 66
4.9 Input for case 2a . . . 67
4.10 Output for case 2a . . . 67
4.11 Input for case 3a . . . 68
4.12 Output for case 3a . . . 68
4.13 Input for case 4a . . . 69
4.14 Output for case 4a . . . 69
4.15 Input for case 1b . . . 70
4.16 Output for case 1b . . . 70
4.17 Input for case 2b . . . 71
4.18 Output for case 2b . . . 71
4.19 Input for case 3b . . . 72
4.20 Output for case 3b . . . 72

4.21 Input for case 4b 73
4.22 Output for case 4b 73
4.23 Input for case 1c 74
4.24 Output for case 1c 74
4.25 Input for case 2c 75
4.26 Output for case 2c 75
4.27 Input for case 1d 76
4.28 Output for case 1d 76
4.29 Input for case 2d 77
4.30 Output for case 2d 77
4.31 AHP Propulsion Trade-off 80

Symbols

a = Semi-major axis

e = Eccentricity

i = Inclination

Ω = Longitude of the Ascending Node

ω = Argumentum of Periapsis

ν = True Anomaly

$\mathbf{T}$ = Time of periapsis passage

c = Effective Exhaust Velocity

I_{sp} = Specific Impulse

I_{tot} = Total Impulse

m_0 = Initial Mass

m_f = Final Mass

m_p = Propellant Mass

m_s = Power Source Mass

m_u = Payload Mass

α = Specific Power Generator Mass

η = Efficiency

β = Technological Level

P_T = Thrust Power

$\vec{B}$ = Magnetic Field

$\vec{E}$ = Electric Field

Acronyms

EMPT	Enhanced Magnetic Plasma Thruster
EP	Electric Propulsion
HET	Hall Effect Thruster
IOSHEXA	In Orbit Servicing HEXAgon
LEO	Low Earth Orbit
MET	Microwave Electrothermal Thruster
SSMS	Small Spacecraft Mission Services
S/C	Spacecraft
TOF	Time Of Flight

Chapter 1

Introduction

One of the most impressive things about looking at recent developments in space launches is the incredible increase in Small Satellites Missions, particularly since 2013. This figure is a clear consequence of the important technological improvements that have characterized these last years and that have allowed small satellites to achieve objectives and the ability to carry out missions that until a few years ago were the prerogative of much larger satellites. Increasingly, smallsats are being used to build and implement large-scale commercial activities ranging from communications to Earth Remote sensing. Based on the opinions of the industry, there is a broad consensus that this trend will not stop in the future but will accelerate and continue to change the world of space.

The launch strategy for these small satellites in Low Earth Orbit (LEO) was at first based on the possibility of *piggyback* travel alongside the so-called primary payloads. This possibility has ensured relatively low-cost access to space also to these systems allowing those who dealt with them to do business on the data collected. Parallel to the spread of *piggyback* launches in recent years, we have witnessed the development of NewSpace launch systems, most of these born from private initiatives with different load capacities (at most a few hundred kilos in LEO). The objective of these new launch systems is to meet the growing demand for access to space in the small satellite market. As the possibilities of using smallsats grow, however, the limits of the current launch possibilities become more and more evident, in particular, satellite operators are harmed by the limits inherently connected to these modalities with negative repercussions on time to mission/market of their products. An example of a limitation in the launch of a satellite "guest" of a primary payload is the impossibility to manage at will the orbital parameters or delays in the launch related to the needs of the main payload and not manageable by the secondary payload [1]. Even more recently, *rideshare* missions have been organized. These missions represent a more effective response to the growing demand for cheap and rapidly available launches for small satellites. As we said, until now these customers have relied on the ability to obtain a 'piggyback' pass along with the main satellite, but space is limited, and matching the requirements of the main mission is often difficult.

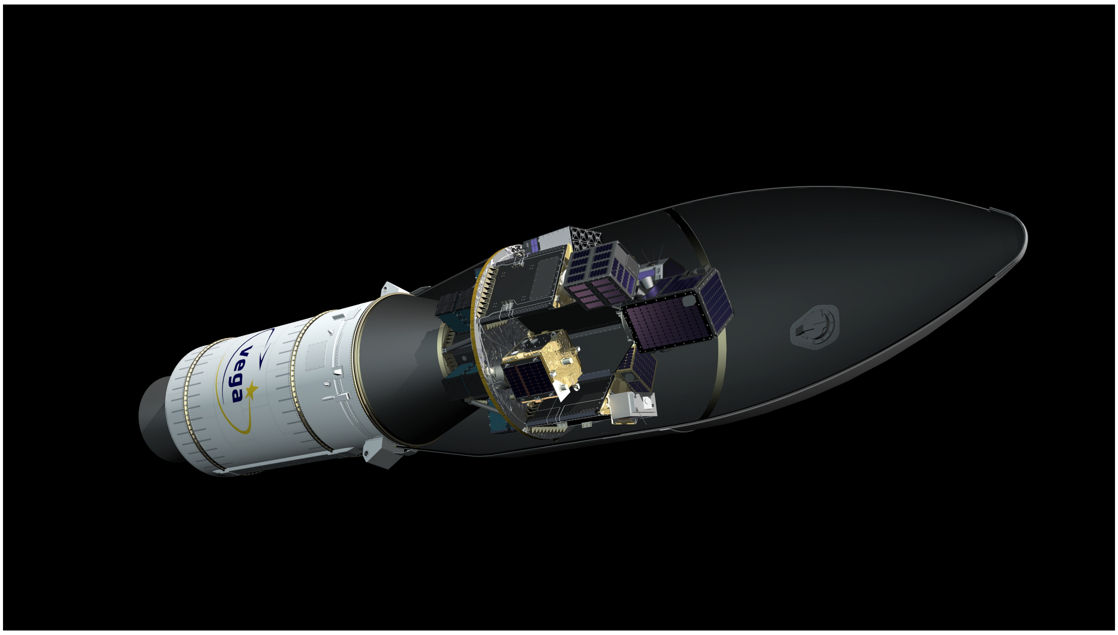

Figure 1.1: Small Spacecraft Mission Services (*SSMS*)

In the strictly European area, an interesting solution is new multiple support, transport, and separation system called SSMS - Small Spacecraft Mission Service 1.1. The SSMS platform makes effective use of all available space through a modular design approach. The lower section is hexagonal and can hold six nano-satellites or up to a dozen CubeSat dispensers. The upper section is used for micro-satellites, mini-satellites, and small satellites. The lower section can also be used independently, paired with a larger satellite that replaces the upper section.

1.1 IOSHEXA concept

Enthusiastic about this new trend, SAB Launch Services (SAB L-S) has started to think about a solution that can improve the offer provided by a typical piggyback configuration of SSMS called HEX-1. The objective is to guarantee to customers who rely on missions of this type as secondary payloads, the same benefits guaranteed to primary payloads, conceptually approaching rideshare and piggyback missions. To pursue this objective the basic idea is to add a propulsion system to the dispenser;

this solution would allow a greater flexibility requireb by small satellites without having to depend on external carriers which provides services not included in the launch capacity costs (e.g. ION) but using the structure of the adapter. On the other hand such a system would allow the integration on the same dispenser of further interesting equipment, if this first demonstration mission with electric propulsion should be successful, with the possibility to carry out several types of applications such as:

- Release and positioning of small satellites
- Debris removal
- Refurbishment
- Refueling
- In-Orbit Manufacturing

Therefore, the whole project is named IOSHEXA - In Orbit Servicing HEXAgon, as the motorization of a hexagonal deployer partially based on what was developed by SAB Aerospace during the design of SSMS for AVIO.

Services elected from Debris Removal are currently being studied internally by SAB L-S. In this thesis we will mainly describe the first service introduced, i.e. "satellite release and positioning", giving instead only brief hints of the reasons why we are interested in debris removal as a strategic objective. The remaining previously introduced services will be evaluated once IOSHEXA and the integrated equipment will have reached a robust Technology Readiness Level - TRL (roughly between 2027 and 2035).

1.1.1 Release and positioning of small-sat

Among the various subsystems that make up a spacecraft, one of the most interesting elements is certainly the propulsion subsystem. A satellite equipped with autonomous propulsion can place itself in the most convenient orbit for the performance of the mission for which it was conceived; of course, the integration of a propulsion system capable of modifying the orbital parameters of the satellite itself brings with it a series of technical complications and disadvantages in terms of volumes involved and additional masses to carry on board, often not acceptable to the producers of small satellites and CubeSats. Therefore, what typically happens today is that satellites once released from the deployer find themselves on a compromise orbit with potential disadvantages in terms of mission effectiveness.

In order to relieve small satellite manufacturers from the design of a propulsion subsystem, IOSHEXA is proposed as a sort of space tug integrated into the launcher able to modify, where necessary, the orbital parameters of the motorized dispenser before the release of the satellites. The maneuvers that can be performed by the deployer are mainly the following three:

- Periaps raising/lowering
- Plane Change
- Phasing

Once the operational orbit of one of the satellites on board the deployer is reached, the satellite concerned is then released and can begin to perform operations to start its mission autonomously.

1.1.2 Debris Removal

The IOSHEXA project has other horizons. The final objective for a system of this type is in-orbit servicing and , in particular, in this paragraph we will better investigate the reasons that led us to design a system capable of performing active *debris removal* operations.

Over half a century of spaceflight activity since the Sputnik-1 mission in 1957 has produced a significant growth in what is now known as "space debris." The term space debris relates to "all man-made objects, including fragments or items that are in Earth orbit and are no longer operational." This considerable population of space debris must be considered in the design of the payload and the mission itself to ensure safe operations with low risk of satellite loss or damage in the case of unmanned missions and to avoid casualties in the case of manned missions.

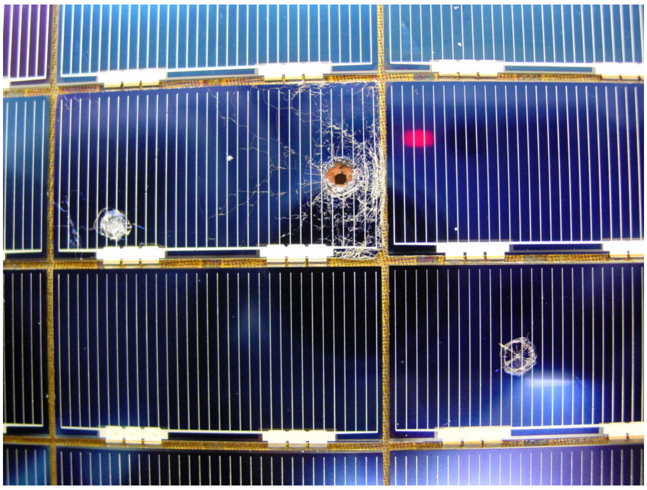

Figure 1.2: ESA built-solar cells retrieved from the Hubble Space Telescope in 2002

To date, our knowledge of the space debris environment is mostly based on ground-based radar and optical surveys. In LEO, most radars provide coverage for objects between 5 cm and 10 cm in size during space surveillance and wheel tracking operations. In GEO orbit, telescopes allow the tracking of objects with dimensions between 30 cm and 1 m. [2] To get an idea of the number and magnitude of space debris in circulation, please refer to the following table 1.1

Table 1.1: Contributions by macro object to the MASTER-2005 model reference population discriminated by size regimes, orbital regions and sources in LEO [2]

Source type	Orbit Regime	> 1 mm	> 1 cm	> 10 cm	> 1 m
Launch/MRO	LEO	4 025	3 214	3 175	2 030
	LEO+MEO+GEO	31 043	5 393	5 354	3 895
Explosions	LEO	$6.42e+6$	183 179	8 714	379
	LEO+MEO+GEO	$1.54e+7$	411 226	15 033	764
Collisions	LEO	23 195	453	124	1
	LEO+MEO+GEO	41 391	775	133	1
NaK	LEO	44 935	24 030	0	0
	LEO+MEO+GEO	44 935	24 030	0	0
SRM slag	LEO	$5.68e+6$	16 905	0	0
	LEO+MEO+GEO	$1.27e+8$	165 493	0	0
Ejecta	LEO	$1.23e+6$	0	0	0
	LEO+MEO+GEO	$3.66e+6$	0	0	0
Total Count	LEO	$1.34e+7$	227 782	12 013	2 409
	LEO+MEO+GEO	$1.47e+8$	606 917	20 520	4 660

A potential means to mitigate the space debris problem is therefore certainly represented by active debris removal (ADR), in particular, such a solution is particularly interesting in low Earth orbit. This solution, already proposed since the '80s, has so far been put aside due to the considerable technical difficulties and high costs. The constant growth in the number of debris, however, requires the search for a solution at any cost, and ADR appears at the moment the only viable solution to preserve the space environment for future generations. The European Space Agency (ESA) has identified the development of technologies for the active removal of debris as a strategic objective to be pursued. ADR is essential to curb the uncontrolled growth of debris. This methodology must however continue to be supported by the adherence of satellite manufacturers to the guidelines imposed by ESA, with particular reference to the orbital decay over 25 years, to avoid further accumulation of debris. At present studies predict that, in the absence of countermeasures, the natural tendency of the space environment will be to increase the number of debris present in LEO orbit. The measures proposed by the Inter-Agency Space Debris Coordination Committee (IADC) will be able to reduce but not stop the growth, even assuming the interruption of all launch activities. This is evidence that the population of large objects has now reached a critical concentration in LEO, which is why mitigation alone is insufficient.

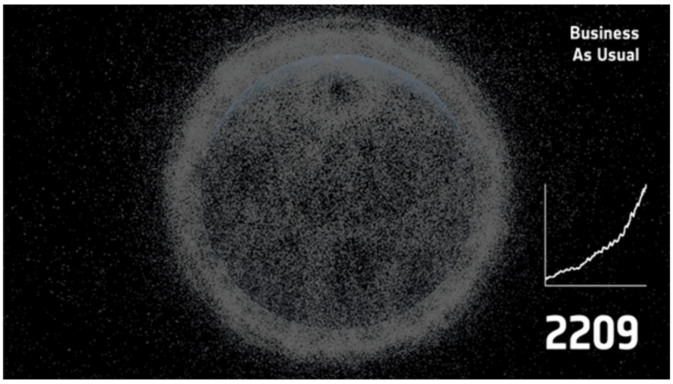

Figure 1.3: Business as Usual

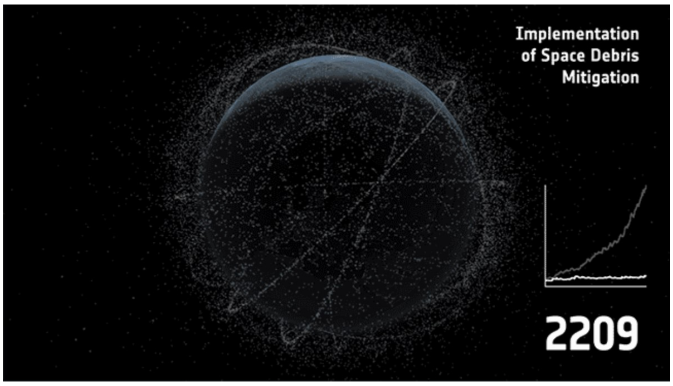

Figure 1.4: Implementation of Space Debris Mitigation

According to an ESA estimate, the LEO environment is currently populated by about 3200 intact objects. Considering an analysis also conducted by ESA, the number of intact objects to have in orbit to bring to 50% the probability of reducing the overall debris population is much lower and equal to 2500 (i.e. the state in the mid-90s). So if such a prospect were to be considered as an attractive target for mitigating the debris problem this would mean that the number of intact objects in orbit must be reduced even while spaceflight activities continue. However, if we look at the data regarding the number of satellites launched in recent years, we realize that this operation is unfeasible, in fact between 2004 and 2012 about 72 objects per year were placed in LEO; between 2013 and 2016, the average number of satellites placed in LEO per year rose to 125 (this is mainly due to the widespread use of small satellites); in 2015, several companies announced their willingness to deploy large constellations with more than 1000 satellites in LEO to provide fast internet worldwide (Starlink, OneWeb, etc). Thus, it is clear that the only option available is to actively remove the large objects that are now in orbit and would be destined to stay in space for even more years. The benefits of this would be several:

- The objects that would generate the most debris in the event of a collision or at the greatest risk of collision could be removed first;
- Satellites that are no longer active could be removed;
- Controlled deorbit would be possible.

To perform this "cleanup" in LEO as efficiently as possible the characteristics of the objects to be removed could be:

1. High mass objects (those with the greatest environmental impact);
2. Objects with a higher probability of collision;
3. Objects at higher altitudes (the fragments following a possible collision would remain in orbit longer).

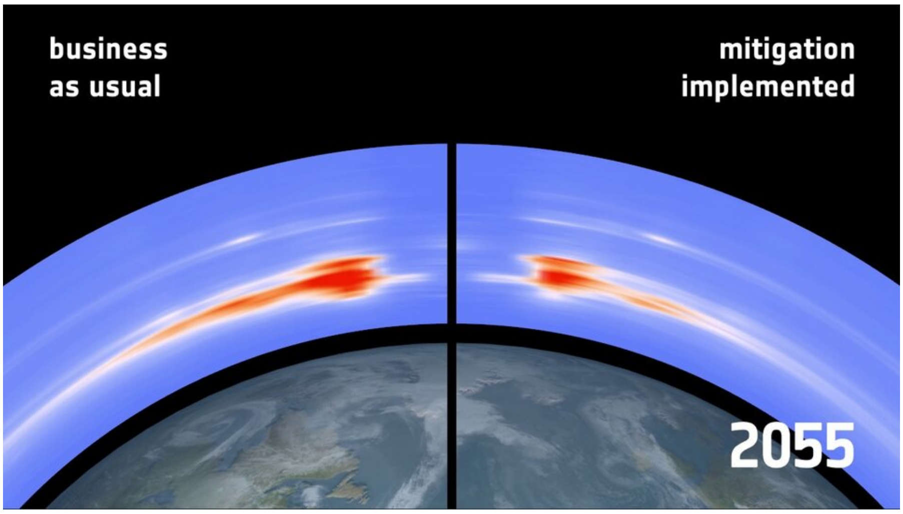

Figure 1.5: Future debris density at poles with and without active debris removal

The most densely populated region of LEO is now between 800 and 1000 km and at high inclinations. In this context three so-called "high-ranking hotspot regions" are identified [3].

- 1000 km and 82º inclination;
- 800 km and 98º inclination;
- 850 km and 71º inclination.

1.1.3 IOSHEXA IOD mission

The mission being presented in the frame of this thesis is the In Orbit Demonstration (IOD) Mission of the In Orbit Servicing HEXA (IOSHEXA). IOSHEXA will perform a first IOD Mission in 2025. The Space Tug will be released by VEGA on a SSO 550 km and it will deploy micro and nanosatellites from three of its six panels. Once all the microsats and cubesats will be released, the tug will increase its altitude to achieve SAFIR-2, which is a OHB satellites that ended its mission on a SSO 823 km orbit.

Table 1.2: Orbits specifications in the IOD mission

	AVUM Initial Circular Orbit	SAFIR-2 Debris Orbit
Altitude [km]	550	823
Inclination [deg]	97.6	98.8
Phase [deg]	0	90

Rendezvous maneuvers will be performed in order to catch the satellite and then performing disassembly of its main components. After final approach, the robotic arm will perform a soft capture of the target and bring it closer to the IOSHEXA. Then the target will be securely berth with the IOSHEXA via a dedicated grapple. Afterwards the robotic arm will change tools, replacing the SAFIR-2 soft capture grapple by a bolting tool. Finally, the robotic arm will unbolt one of the booms of SAFIR-2, retrieving and storing the boom. Once the demonstrative on-orbit service will be performed, IOSHEXA will deorbit to a lower orbit to be compliant with the ESA Space Debris Mitigation. This will be a demonstrative mission to validate the robotics and the performances of IOSHEXA in terms of in-orbit servicing. In particular, its robotic arm could be used for such a mission, but also for missions that could involve recycling and assembly of targeted spacecrafts. Indeed, IOSHEXA could be seen as a valid transport for micro and nanosatellites, but also as a valid carrier which is able to improve the space environment, though support to other satellites and a means of recycling. Future missions are foreseen, where the new concepts of the IOSHEXA will be able to "help" satellites in LEO and GEO orbits. In particular, new missions aim to perform refueling and refurbishment. Once the TRL of the other instruments will be able to be integrated into the Space

Tug, IOSHEXA will be able to perform in a range of 2027- 2035 also other missions also for in-orbit manufacturing.

Chapter 2

Fundamentals of Astrodynamics

This chapter reviews some notions in orbital mechanics and presents a brief treatment of the vast field of astrodynamics [4].

2.1 Keplerian Orbits

Kepler's laws are three laws concerning the motion of the planets. They are Johannes von Kepler's main contribution to astronomy and mechanics [4].

- *First Law*: "The orbit of each planet is an ellipse, with the sun at a focus"
- *Second Law*: "The line joining the planet to the sun sweeps out equal areas in equal times"
- *Third Law*: "The square of the period of a planet is proportional to the cube of its mean distance from the sun"

2.1.1 Newton's Laws

Kepler's laws represent only one description of the motion of the planets. The theoretical basis will then be provided by Sir Isaac Newton and the laws contained in the first book of the "*Principia*"[4].

- *First Law*: "Every body continues in its state of rest or of uniform motion in a straight line unless it is compelled to change that state by forces impressed upon it"

- *Second Law*: "The rate of change of momentum is proportional to the force impressed and is in the same direction as that force"
- *Third Law*: "To every action there is always opposed an equal reaction"

A mathematical expression for the second law can be as follows:

$$\sum \vec{F} = m\ddot{\vec{r}} \tag{2.1}$$

2.1.2 Two-body problem

In the principia Newton also gave formulation of the law of universal gravitation asserting that two bodies attract with a force $\vec{F_g}$ which can be expressed mathematically as:

$$\vec{F_g} = -\frac{Gm_1m_2}{r^2}\frac{\vec{r}}{r} \tag{2.2}$$

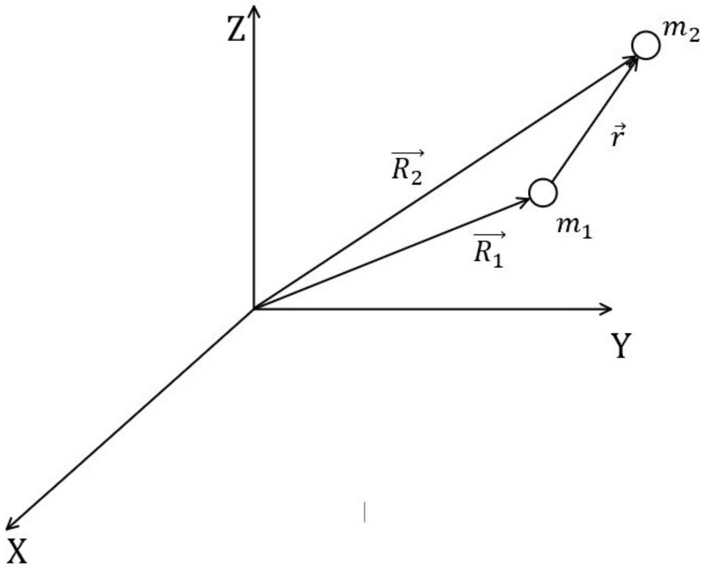

Figure 2.1: Representation of the generic two-body problem in an Inertial Reference Frame

where

- $\vec{F_g}$ is the force acting on mass m_2 due to mass m_1
- $\vec{r}$ is the vector joining the two material points of mass m_1 and m_2 with direction $m_1 - m_2$

- G is the universal gravitational costant with the value $6.67 \times 10^{-11} \frac{Nm^2}{kg^2}$

If we rename m_2 as m, to indicate the mass of the S/C and m_1 as M, to indicate the mass of the earth, and adapting to this new nomenclature also the respective position vectors (R_1 becomes ρ and R_2 becomes R) and the vector difference $\vec{R}$-$\vec{\rho}$ is indicated with $\vec{r}$, then the law of universal gravitation becomes:

$$\vec{F_g} = -\frac{GMm}{r^2}\frac{\vec{r}}{r} \tag{2.3}$$

2.1.3 Two-body equation of motion

Consider the following three simplifying assumptions to be valid:

1. The two bodies considered are characterized by both spherical and mass symmetry. This allows the bodies to be treated as point masses.

2. The mass of the spacecraft m is much smaller than the mass of the earth M.

3. Only gravitational forces act on the system.

Under these assumptions, Newton's second law of motion combined with the law of universal gravitation returns us the equation for the satellite acceleration vector or *two-body equation of motion*:

$$\ddot{\vec{r}} + (\mu r^{-3})\vec{r} = 0 \tag{2.4}$$

Where $\mu \equiv GM$ is, in this case, the Earth's gravitational constant (equal to 398600.5 km^3/sec^2).. Starting from this relation it is possible to obtain, with some steps, the equation of the trajectory. Before explaining the latter, we make some considerations of kinematic nature; to do this we introduce a polar coordinate system.

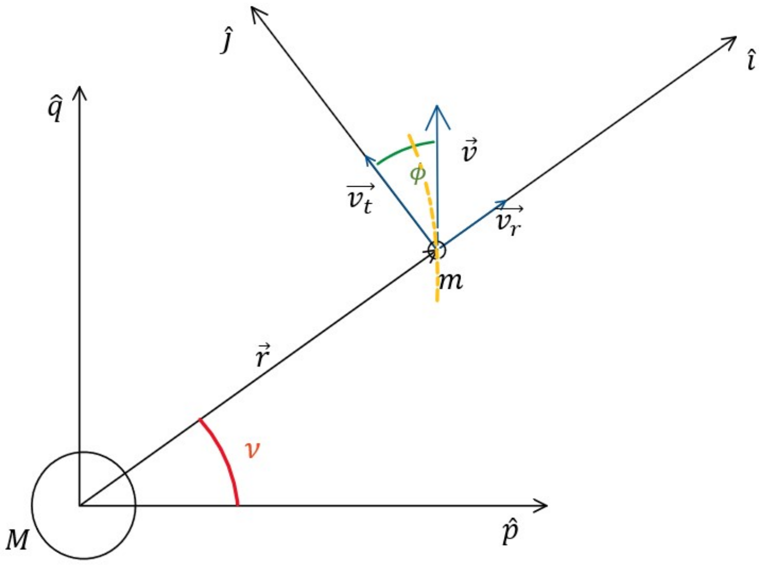

Figure 2.2: Two-body problem in a polar coordinate system

In figure 2.2 we can observe a representation of the vectors $\vec{r}$ and $\vec{v}$ in the orbital plane. Two reference systems are represented with non-rotating polar $\widehat{p}$-$\widehat{q}$ and rotating $\widehat{i}$-$\widehat{j}$ where

$$\begin{cases} \widehat{i} = \widehat{p}\cos\nu + \widehat{q}\sin\nu \\ \widehat{j} = -\widehat{p}\sin\nu + \widehat{q}\cos\nu \end{cases} \tag{2.5}$$

In these reference systems we can distinguish two important angles:

1. ϕ called *flight path angle*
2. ν called *true anomaly.*

We can also decompose in reference $\widehat{i}$-$\widehat{j}$ the velocity vector $\vec{v}$ into two components:

- $\vec{v_t}$ called *tangent component*
- $\vec{v_r}$ called *radial component.*

We can therefore express in the reference $\widehat{i}$-$\widehat{j}$

$$\vec{r} = \begin{cases} r \\ 0 \end{cases} \qquad \vec{v} = \dot{\vec{r}} = \begin{cases} \dot{r} \\ r\dot{\nu} \end{cases} \qquad \vec{a} = \ddot{\vec{r}} = \begin{cases} \ddot{r} - r\dot{\nu}^2 \\ 2\dot{r}\dot{\nu} + r\ddot{\nu} \end{cases} \tag{2.6}$$

2.1.4 Constants of the motion

From equation 2.4 we can derive a series of quantities called *constants of motion* of a satellite in orbit.
We introduce then the **specific mechanical energy** defined as follows:

$$E_g = \frac{v^2}{2} - \frac{\mu}{r} \tag{2.7}$$

This represents the mechanical energy per unit mass and is the sum of the kinetic energy per unit mass and the potential energy per unit mass. The equation 2.7 is also known as *energy equation*.

It is possible to demonstrate, with some simple steps that in the following we will leave out in order not to burden the discussion, that there is another constant, the **specific angular momentum** and it is defined as:

$$\vec{h} = \vec{r} \times \vec{v} \tag{2.8}$$

It follows that the specific angular momentum $\vec{h}$, since it is defined as a cross product between $\vec{r}$ and $\vec{v}$, is itself a **costant vector**, so that $\vec{r}$ and $\vec{v}$ must always lie in the same plane. For this reason, the motion of the satellite is confined in a plane, called *orbital plane*, that is fixed in space. Using the expression h as a cross product we can then write:

$$h = rv\ \sin(90° - \phi) = rv\ \cos\phi \tag{2.9}$$

2.1.5 The trajectory equation

By integrating equation 2.4 we obtain the **trajectory equation**:

$$r = \frac{h^2/\mu}{1 + (B/\mu)\ \cos(\nu)} \tag{2.10}$$

where:

- $\vec{B}$ is the vector constant of integration pointing in the direction of the periapsis;
- ν is the angle measured from $\vec{B}$ to $\vec{r}$, it is therefore evaluated from the periapsis.

The expression of r at equation 2.10 is related to the concepts of dynamics and kinematics. A geometric expression in polar coordinates is as follows:

$$r = \frac{p}{1 + e\ \cos(\nu)} \tag{2.11}$$

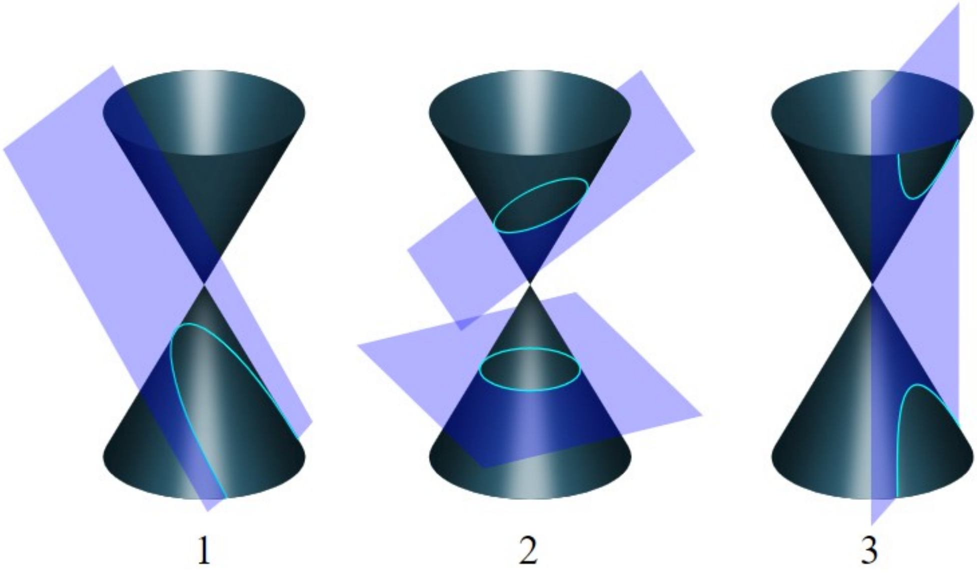

Figure 2.3: Conic sections

Equation 2.11 is the equation of a conic section where:

- p is the so called *semilatus rectum*;
- e is the *eccentricity* which determines the type of conic section.

In the table 2.1 we indicate some geometric generalities common to all the sections of conic

Table 2.1: Geometrical properties common to all conic sections

Property	Description	Expression
e	Eccentricity	$\frac{c}{a}$
p	Semilatus Rectum	$a(1-e^2)$
r_p	Radius of periapsis	$\frac{p}{1+e}$
r_a	Radius of apoapsis	$\frac{p}{1-e}$

Elliptical Orbit

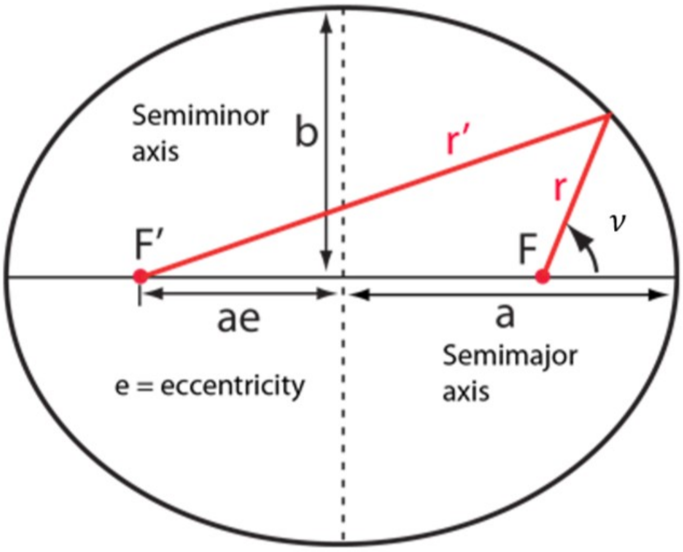

Figure 2.4: Elliptical Orbit

All planets in the solar system and all satellites orbiting the earth are characterized by elliptical orbits. Some characteristic geometric properties of this particular orbit are given below.
The major axis of an elliptical orbit is equal to:

$$r + r' = 2a \tag{2.12}$$

An alternative mathematical relationship is (with r_a *radius of apoapsis* and r_p *radius of periapsis*):

$$r_a + r_p = 2a \tag{2.13}$$

An expression for the distance between the two foci is instead:

$$r_a - r_p = 2c \tag{2.14}$$

So putting in relation the eq. 2.14 with the eq. 2.13 it results:

$$e = \frac{r_a - r_p}{r_a + r_p} \tag{2.15}$$

Finally, it is possible to demonstrate, starting from the expression of h given in eq. 2.9 and using the elementary calculus, that the **period of an elliptical orbit** is

$$\mathcal{T}_E = \frac{2\pi}{\sqrt{\mu}} a^{3/2} \tag{2.16}$$

Circular Orbit

When the eccentricity of the conic is zero (e = 0), the orbit in question is called *circular orbit.* This is a particular case of elliptical orbit for which the radius of the periapsis coincides with the radius of the apoapsis.

$$r_p = r_a \tag{2.17}$$

In this case the expression for the period of the orbit becomes:

$$\mathcal{T}_C = \frac{2\pi}{\sqrt{\mu}} r^{3/2} \tag{2.18}$$

Table 2.2: Relating E_g to the geometry of an orbit [5]

Conic	Energy, E_g	Semi-major axis, a	Eccentricity, e
Circle	<0	=radius	0
Ellipse	<0	>0	$0 < e < 1$
Parabola	0	∞	1
Hyperbola	>0	<0	>1

2.1.6 Classical Orbital Elements

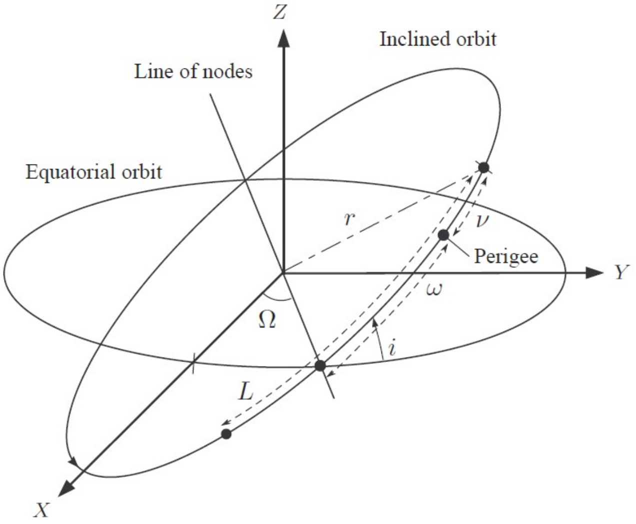

Figure 2.5: Classical Orbital Elements [6]

In order to fully determine the size, shape, and orientation of an orbit, five independent quantities known as *orbital elements* are sufficient.
To then localize a particular position of the satellite at a given instant of time, a sixth element is introduced. The table below defines and describes the *classical orbital elements*.

Table 2.3: Classical Orbital Elements

Symbol	Orbital Element	Description
a	Semi-major axis	A costant defining the size of the conic orbit.
e	Eccentricity	A costant defining the shape of the conic orbit.
i	Inclination	The angle between the $\widehat{K}$ unit vector (versor of the $\vec{Z}$ axis in fig. 2.5) and the angular momentum vector $\vec{h}$ (normal to the orbit).
Ω	Longitude of the Ascending Node	the angle in the fundamental plane, between the $\widehat{I}$ unit vector (versor of the $\vec{X}$ axis in fig. 2.5) and the point where the satellite crosses through the fundamental plane in a northerly direction (ascending node) measured counterclockwise when viewed from the north side of the fundamental plane.
ω	Argumentum of periapsis	The angle, in the plane of the satellite's orbit, between the ascending node and the periapsis point, measured in the direction of the satellite's motion.
ν	True anomaly	The angle from the eccentricity vector to the satellite position vector, measured in the direction of satellite motion.
T	Time of periapsis passage (alternative to ν)	The time when the satellite was at periapsis.

It should be noted that often as an alternative element to the semi-major axis it is preferred to use the *semilatus rectum p*.
Circular orbits ($e = 0$) and equatorial orbits ($i = 0$) require the definition of alternative orbital parameters since the classical orbital elements are undefined.
In case of orbits with $i = 0$ we introduce the *longitude of periapsis*: $\Pi = \Omega + \omega$.
In case of orbits with $e = 0$ we introduce the *argument of latitude*: $u = \omega + \nu$.
Finally in case of orbits with $e = 0$ and $i = 0$ we introduce the *true longitude*: $l = \Omega + \omega + \nu = \Pi + \nu = \Omega + u$.

2.2 Orbital Maneuvers

During the lifetime of our satellites, all these objects will need to perform orbital maneuvers to modify one of the orbital elements. Typically the maneuvers to be performed will be aimed to change the altitude of the orbit, the orbital plane, or both, this can be done by changing the velocity vector in modulus or direction. Typically the burn times compared with the characteristic times of the orbit are much lower, so the maneuvers can be assumed as impulsive in the case of chemical propulsion. The different discussions will be done for electric propulsion. In general we can say that the velocity variation to be provided for the generic maneuver is [5]:

$$\Delta V = V_{NEED} - V_{CURRENT} \tag{2.19}$$

2.2.1 Adjustment of Periapsis and Apoapsis Height

Adjusting the height of Periapsis and Apoapsis falls under the umbrella of so-called *In-Plane Orbit Changes*.

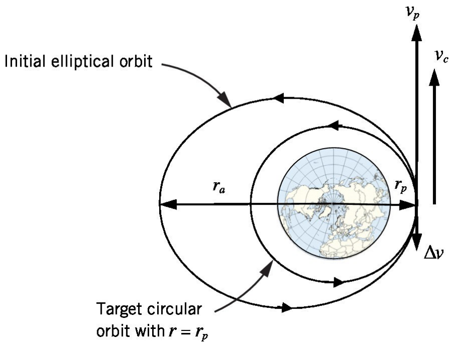
v_p
v_c
Initial elliptical orbit
r_a
r_p
Δv
Target circular orbit with $r = r_p$

Figure 2.6: Apoapsis Lowering [7]

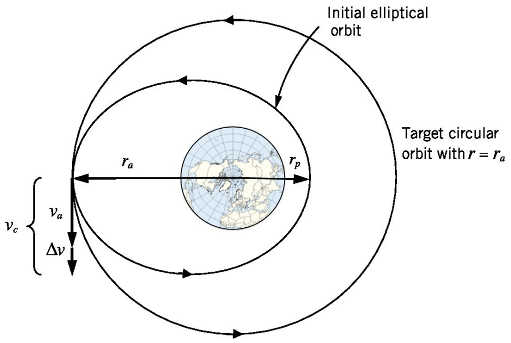
Initial elliptical orbit
Target circular orbit with $r = r_a$
r_a
r_p
v_c
v_a
Δv

Figure 2.7: Periapsis Raising [7]

If we consider the expression for the total specific mechanical energy of eq. 2.7 and make a number of considerations bearing in mind the definitions collected in tab. 2.1 we obtain a relation on the energy valid for all orbits:

$$E_g = \frac{v^2}{2} - \frac{\mu}{r} = -\frac{\mu}{2a} \tag{2.20}$$

Solving for v^2 we obtain:

$$v^2 = \mu\left(\frac{2}{r} - \frac{1}{a}\right) \tag{2.21}$$

Supposing to change the velocity, v, leaving r unchanged we have:

$$2vdv = \frac{\mu}{a^2}da <=> da = \frac{2a^2}{\mu}vdv \tag{2.22}$$

We then observe that if we provide an infinitesimal change in velocity dv then we get an infinitesimal change in the semi-major axis da.
Providing a ΔV to the apoapsis results in an altitude change to the periapsis; similarly providing a ΔV to the periapsis results in an altitude change to the apoapsis. In formulas:

$$\Delta h_a \approx \frac{4a^2}{\mu}v_p\Delta v_p \tag{2.23}$$

$$\Delta h_p \approx \frac{4a^2}{\mu}v_a\Delta v_a \tag{2.24}$$

2.2.2 The Hohmann Transfer

Also in the context of In-plane Orbit Maneuvers, a particular type of maneuver known as a "Hohmann Transfer" will be described below. The maneuver in question is the one that requires the least amount of DV to perform the transfer between two circular orbits, a transfer that is obtained by placing the satellite on an elliptical, bitangent transfer orbit.

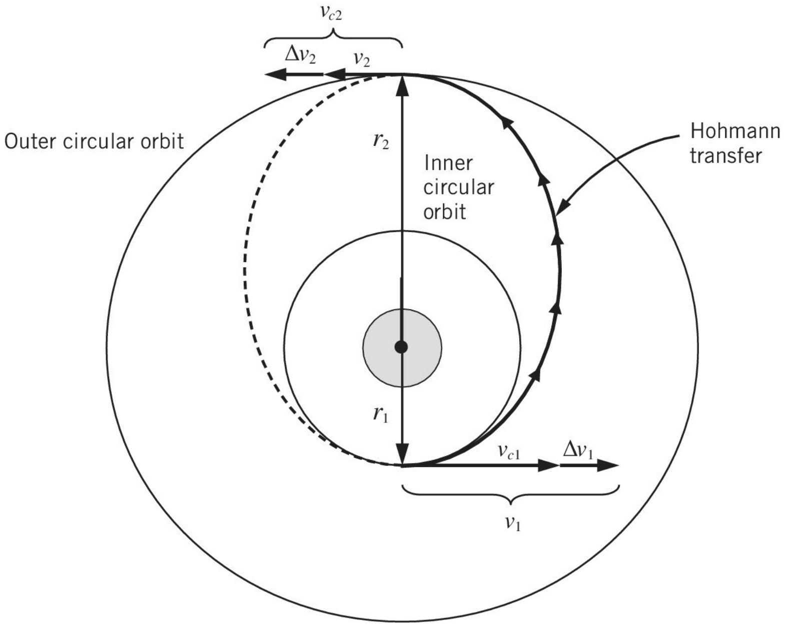

Figure 2.8: Hohmann Transfer [7]

Suppose we want to travel along the transfer orbit to move from the smallest circular orbit of radius r_1 to the largest circular orbit of radius r_2.
The transfer orbit is an elliptical orbit with major axis equal to:

$$2a_t = r_1 + r_2 \tag{2.25}$$

Since the total specific mechanical energy is $E_g = -\frac{\mu}{2a}$ then:

$$E_t = -\frac{\mu}{r_1 + r_2} \tag{2.26}$$

Writing the expression of the energy at the periapsis of the transfer orbit (point 1) and making v_1 explicit we get:

$$v_1 = \sqrt{2\left(\frac{\mu}{r_1} + E_t\right)} \tag{2.27}$$

Since the satellite is on a circular orbit it is characterized by a speed equal to $v_{cs1} = \sqrt{\frac{\mu}{r_1}}$, we have to provide an increase of speed equal to:

$$\Delta v_1 = v_1 - v_{cs1} \tag{2.28}$$

The same criterion can be applied to evaluate the Δv to be provided at point 2 where the satellite will arrive with a velocity v_2.

The duration of the transfer also called *time of flight* can be evaluated by taking into account that the Hohmann transfer takes place on a semi-ellipse, reasoning that, known a_t, the TOF is equal to 1/2 of the period of the ellipse:

$$TOF = \pi\sqrt{\frac{a_t^3}{\mu}} \tag{2.29}$$

It should be noted that while the Hohmann transfer turns out to be the least ΔV-intensive, it also turns out to be the slowest of the two-impulse transfer orbits.

2.2.3 General Coplanar Transfer

Another *In-Plane maneuver* of interest is the generic coplanar transfer orbit; in this case, we will present a transfer between two circular orbits. As we can deduce from what was said in the previous paragraph, this maneuver will certainly be more ΔV-intensive but faster than the Hohmann transfer.
For such a maneuver to be successful it is obvious that the two thrust points of the generic transfer orbit must intersect or at least touch both the departure and arrival

orbits (in case of tangency to the two orbits we return to the previous limiting case of Hohmann transfer). Mathematically this condition can be expressed with a system of inequalities

$$\begin{cases} r_p = \dfrac{p}{1+e} \leq r_1 \\ \\ r_a = \dfrac{p}{1-e} \geq r_2 \end{cases} \tag{2.30}$$

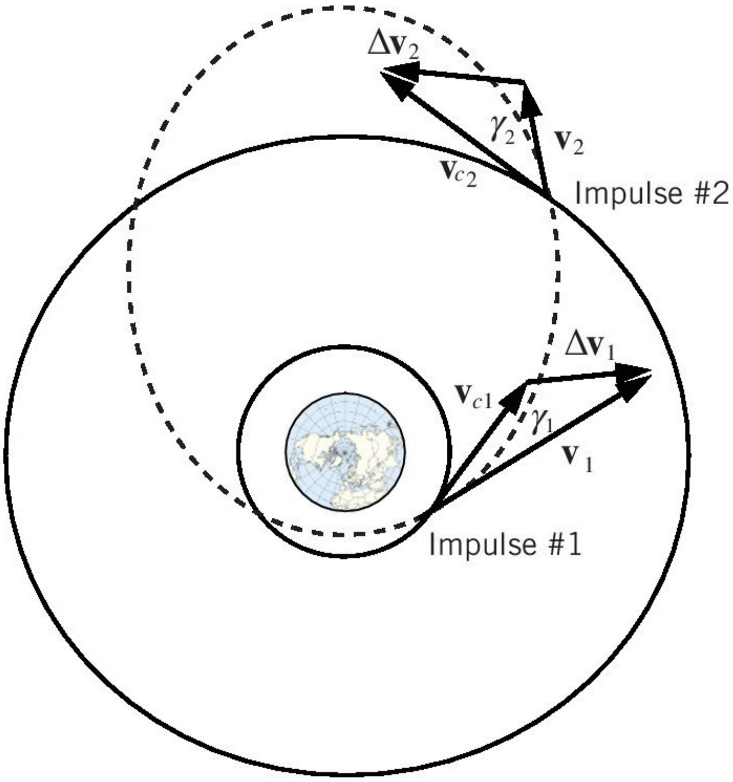
$\Delta\mathbf{v}_2$
γ_2
$\mathbf{v}_2$
$\mathbf{v}_{c2}$
Impulse #2
$\Delta\mathbf{v}_1$
$\mathbf{v}_{c1}$
γ_1
$\mathbf{v}_1$
Impulse #1

Figure 2.9: Coplanar Transfer [7]

Graphing the two inequalities 2.30 yields fig. 2.10

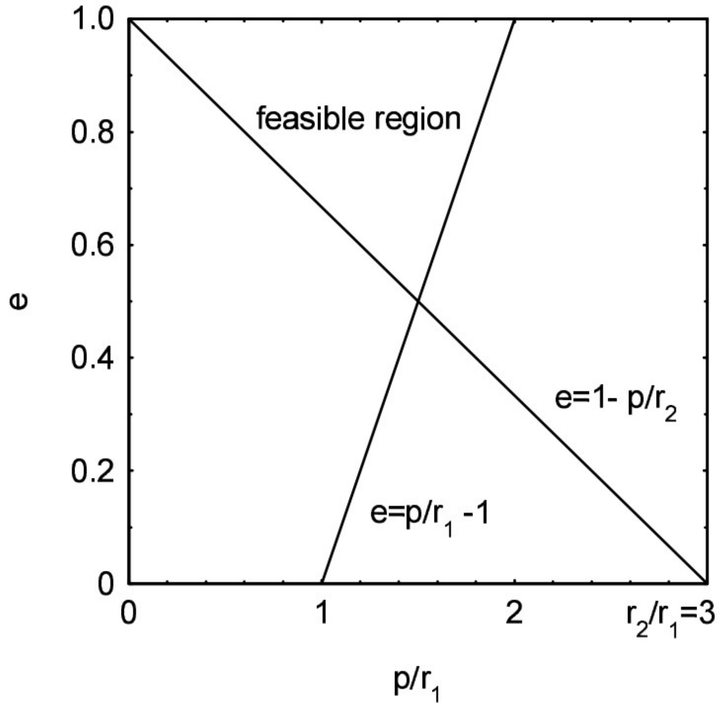

Figure 2.10: p versus e [8]

Assuming we are in the feasibility region and therefore have some p and some e such that the condition given by 2.30 is satisfied, we can write that since $E_t = -\dfrac{\mu}{2a}$ and $p = a(1 - e^2)$ then

$$E_t = -\frac{\mu(1 - e^2)}{2p} \tag{2.31}$$

Furthermore since $p = \dfrac{h^2}{\mu}$ results:

$$h_t = \sqrt{\mu p} \tag{2.32}$$

So, just as we did for the Hohmann Transfer, we can solve the energy equation:

$$v_1 = \sqrt{2\left(\frac{\mu}{r_1} + E_t\right)} \tag{2.33}$$

At point 1, our satellite has circular velocity equal to:

$$v_{cs1} = \sqrt{\frac{\mu}{r_1}} \tag{2.34}$$

So, since the angle between v_{cs1} and v_1 is γ_1, which is the *flight path angle* ϕ_1, we can evaluate it from eq. 2.9 obtaining:

$$\cos\phi_1 = \frac{h_t}{r_1}v_1 \tag{2.35}$$

So, using the law of cosines to solve the third side, ΔV:

$$\Delta v^2 = v_1^2 + v_{cs}^2 - 2v_1v_{cs1}\cos\phi_1 \tag{2.36}$$

Thus, it can be observed that the Hohmann Transfer is only a special case with $\phi_1 = 0; r_p = r_1; r_a = r_2$

2.2.4 Orbit Rendezvous

Up to now, we have all considered maneuvers involving a single satellite. However, satellites often need to carry out maneuvers that can bring them angularly closer to a target, to rendezvous with or intercept another object in orbit. For the maneuver to be successful it is, therefore, necessary that the two objects in question arrive at the meeting point at the same time, and this is possible by setting up what is known as *phasing*. In particular, any orbit followed by the chaser satellite to reach a target satellite or a target space object is defined as *phasing orbit*.

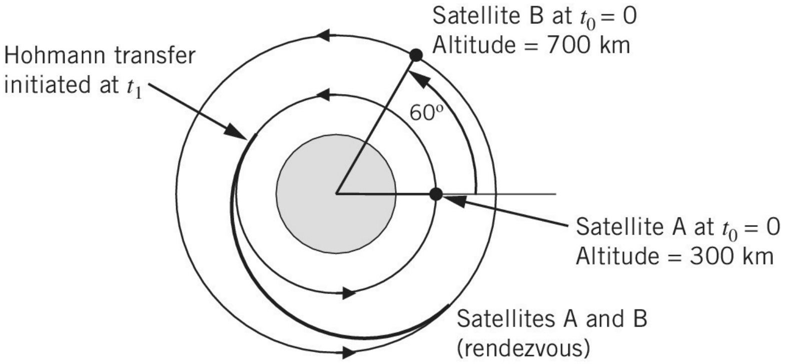

Figure 2.11: Rendezvous Example [7]

Let us consider two satellites A and B placed on two concentric and coplanar circular orbits, and we want to reach satellite B (target) with satellite A (chaser). The phasing orbit is in this case simply the chaser orbit, so we want to inject B into a transfer orbit, typically an Hohmann Transfer.
We need to solve the so-called *Wait Time Equation*:

$$\mathcal{T}_W = \frac{\phi_i - \phi_f + 2k\pi}{\omega_{chs} - \omega_{tgt}} \tag{2.37}$$

where:

- ω_{chs} is the angular velocity of the chaser
- ω_{tgt} is the angular velocity of the target
- ϕ_f is the phase angle and is equal to $180deg - \omega_{tgt} \times TOF_{Hohmann}$
- ϕ_i is the initial phase angle
- k is the number of rendezvous possibilities

If we want the to calculate the total rendezvous time we have to add to WT obtained in 2.37 the TOF of the Hohmann Transfer. We can observe that the denominator in eq. 2.37 is the *relative motion* between chaser and target, so the wait time approaches to infinity if the size of the two orbit is the same. In this case the chaser has to enter a new phasing orbit to reach the target. In case of circular orbits a usefull relation to calculate the drift rate R_D and the required ΔV is [5]:

$$R_D = \Delta\vartheta/((\Delta t * 24 * 60 * 60)/(2\,\pi\sqrt{\frac{r^3}{\mu}}) \tag{2.38}$$

where Δt is the duration in days, and $\Delta\vartheta$ is the angular distance considered,

$$\Delta V = 2\,R_D\,v_c\,1000/1080 \tag{2.39}$$

where R_D is in [Deg/Orbit]

2.2.5 Orbit Plane Changes

We have dealt with maneuvers able to change shape and size of the orbit remaining in the same plane. In order to change orbital plane it is necessary to introduce the so called out-of-plane maneuvers.

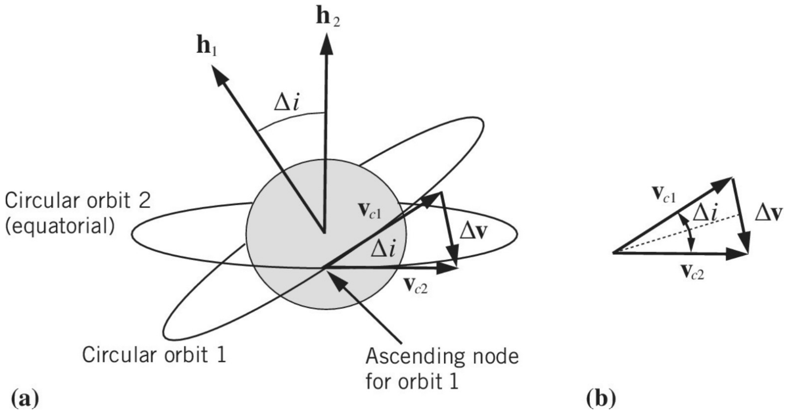
$\mathbf{h}_1$
$\mathbf{h}_2$
Δi
Circular orbit 2 (equatorial)
$\mathbf{v}_{c1}$
$\Delta\mathbf{v}$
Δi
$\mathbf{v}_{c2}$
Circular orbit 1
Ascending node for orbit 1
(a)
$\mathbf{v}_{c1}$
Δi
$\Delta\mathbf{v}$
$\mathbf{v}_{c2}$
(b)

Figure 2.12: Simple Plane Change [7]

If we provide a ΔV in perpendicular direction to the orbit plane we obtain a variation of two orbital parameters, Ω and i; in order to vary only the inclination of the orbit plane we must provide thrust only to the descending node or ascending node.
In this case the following equation is valid for the calculation of the DV to be supplied:

$$\Delta V = 2v \sin \frac{\Delta i}{2} \tag{2.40}$$

This is called the *Simple Plane Change* maneuver since it assumes that the size of the orbit remains constant. It is however an extremely onerous maneuver in terms of ΔV and does not change the E_g of the orbit, in order to optimize the mission we tend therefore to combine this maneuver with other maneuvers, the most typical of which involves raising/lowering the altitude and changing the inclination; this is a more efficient method called *Combined Plane Change.*

$$\Delta v = \sqrt{v_i^2 + v_f^2 - 2v_i v_f \cos \Delta i} \tag{2.41}$$

Chapter 3

Electric Propulsion

All of the orbital maneuvers presented in Chapter 2 used impulsive velocity changes. Our basic assumption is that firing a high-thrust chemical rocket will change the velocity (and hence the orbital elements) instantaneously without any change in position. A very different mode of propulsion is low-thrust propulsion, in which plasmas or charged particles are accelerated using electrostatic or electromagnetic forces and ejected at very high exhaust velocities. Ion and hall effect thrusters are two examples of electric propulsion (EP) devices now used for space missions.The high ep discharge velocities result in specific impulses (I_{sp}) that are nearly 10 times larger than classical chemical rockets. The rocket equation, of which we anticipate one of the results , shows that increasing I_{sp} significantly reduces the propellant mass. However, because the EP mass flow rate is very small, the thrust amplitude is extremely low. as a result, an EP device has to operate continuously so that the very low thrust acceleration produces a considerable velocity (or orbital) change when integrated over a long period (often days or months). We will show the fundamental equation relating ep thrust to electrical power and I_{sp} . Analyzing low-thrust trajectories is challenging because the Keplerian motion of the two bodies is no longer valid and thus the orbital elements change continuously over time when thrust is applied. In EP, a small propulsive force acts continuously on the satellite to slowly increase the altitude (and energy) of the internal orbit until the target orbit is reached. Thus, the orbit transfer is a spiral trajectory that takes place in which each orbital revolution is a nearly circular orbit. An on-board electric propulsion system (such as an ion thruster or hall effect thruster) provides the small, continuous thrust amplitude for the low-thrust transfer. Characterizing a low-thrust transfer is more difficult than analyzing an impulsive orbital transfer because the orbital elements are constantly changing and thus we cannot use the constants of motion (such as E_g and h) to define the transfer orbit between the two circular orbit [7].

3.1 Generalities of space propulsion

It is possible to classify the types of propulsion according to the source from which the energy is obtained and/or the type of acceleration:

- *Chemical propulsion*:characterized by relatively high thrust/weight ratio ;
- *Electrical propulsion*: characterized by an extremely low thrust/weight ratio and high effective exhaust velocities.

Where *propulsion* refers to the **thrust** produced to move a system in a given direction; an acceleration is produced that acts on the initial velocity v_0

Thrust

The thrust is essentially associated with an exchange of momentum with an external body, physically it should therefore be traced back to the principle of action-reaction that in a 1D model leads us to the following formulation:

$$m\frac{dv}{dt} = \dot{m}_p c \tag{3.1}$$

where c is the *effective exhaust velocity.*
This relation is analogous to Newton's law, only in this case m is time-varying, the analyzed system being a variable mass system. The force received by the body is in the opposite direction to that in which the propellant is ejected.
So, we can observe that the body undergoes a variation of mass:

$$\frac{dm}{dt} = -\dot{m}_p \tag{3.2}$$

where $\dot{m}_p$ is the *mass flow rate.*
Therefore making the thrust appear in eq. 3.1 we obtain:

$$T = \dot{m}_p c \tag{3.3}$$

Thrust Power

In order to eject the propellant with a velocity c some energy will be required. We evaluate the energy per unit time:

$$P_T = \frac{1}{2}\dot{m}_p c^2 = \frac{T\,c}{2} \tag{3.4}$$

Total Impulse

To evaluate the cumulative effect of thrust over time:

$$I_t = \int_{t_0}^{t_f} T \, dt \tag{3.5}$$

Eq. 3.5 if we assume that the thrust T is constant reduces to:

$$I_t = T \, \Delta t \tag{3.6}$$

Given an effect (i.e., an I_t), we can get it with high T and small Δt or vice versa. We would like, however, to also include the effects of mass variation Δm, because they too determine the ΔV.

Total propellant consumption

It does not take into account the effects of mass variation.To fill this gap, propellant consumption can be calculated:

$$m_p = \int_{t_0}^{t_f} \dot{m}_p \, dt \tag{3.7}$$

That assuming the mass flow rate remains constant becomes:

$$m_p = \dot{m}_p \, \Delta t \tag{3.8}$$

Specific Impulse

The specific impulse $I_{sp}[sec]$ represents, together with the T-thrust, the most important quantity in space propulsion.It is defined as follows:

$$I_{sp} = \frac{I_t}{m_p \, g_0} \tag{3.9}$$

where $m_p \, g_0$ represents the propellant weight at sea level, on Earth (hypotetical). We can consider I_{sp} as the ratio between effect and cost, in fact it provides the ratio between the actual thrust obtained, represented by the total impulse, and the mass required to obtain it:

$$\frac{\text{effect of thrust}}{\text{weight of propellant consumed}}$$

The I_{sp} is therefore a measure of how effectively the propellant is being utilized. If we assume that T and $\dot{m}_p$ are constant then:

$$I_{sp} = \frac{T\,\Delta T}{\dot{m}_p\,\Delta T\,g_0} = \frac{c}{g_0} \tag{3.10}$$

It is interesting to propose also another interpretation of the quantity I_{sp}, it can in fact be interpreted as a characteristic time, or as the period of time for which an assigned mass of propellant is able to provide a thrust equal to its weight at sea level. Observing that $\dot{m}_p \Delta T$ is just m_p and rearranging eq. 3.10 we get a time of self-sustaining, sea level, equal to I_{sp}:

$$\Delta t = I_{sp} \frac{\cancel{m_p g_0}}{\cancel{T}} \tag{3.11}$$

From eq. 3.9 we can finally observe that the amount of propellant required decreases as the specific impulse increases, and this implies less weight and therefore less cost of the mission.
This result is a consequence of the fact that, in essence, high I_{sp} allows to increase the time during which it is possible to guarantee the same thrust with the same amount of propellant.

3.1.1 Rocket Equation

The objective of a maneuver is to change the velocity of the S/C, i.e. to provide a certain ΔV, understood as the velocity change that the thruster is able to provide. These velocity changes are then ideally related to the thrust and masses involved by the following relationship [8]:

$$\Delta v = \int_{t_0}^{t_f} \frac{T}{m}\,dt \tag{3.12}$$

Equation 3.12 represents the ideal change in velocity that the thruster would provide assuming a single force acting, namely thrust, and parallel to the velocity. Recalling relation 3.3, by performing a change of variables from $\dot{m}_p = -\frac{dm}{dt}$ and assuming $c = cost$, we can obtain by integration the relation identified by Tsiolkovsky and known as *Rocket Equation*:

$$\Delta v = c\,\ln\,(\frac{m_0}{m_f}) \tag{3.13}$$

Starting from eq. 3.13 we obtain a formula widely used in propulsion:

$$\frac{m_f}{m_0} = \exp\left(-\frac{\Delta v}{g_0\,I_{sp}}\right) = \exp\left(-\frac{\Delta v}{c}\right) \tag{3.14}$$

3.1.2 Velocity Losses

Eq. 3.13 and 3.14 represent the ideal velocity changes that the motor would provide under the assumptions of the above described. However, reality is very different and in the calculation of speed jumps it is necessary to take into account the so called *velocity losses*. They are basically of three types:

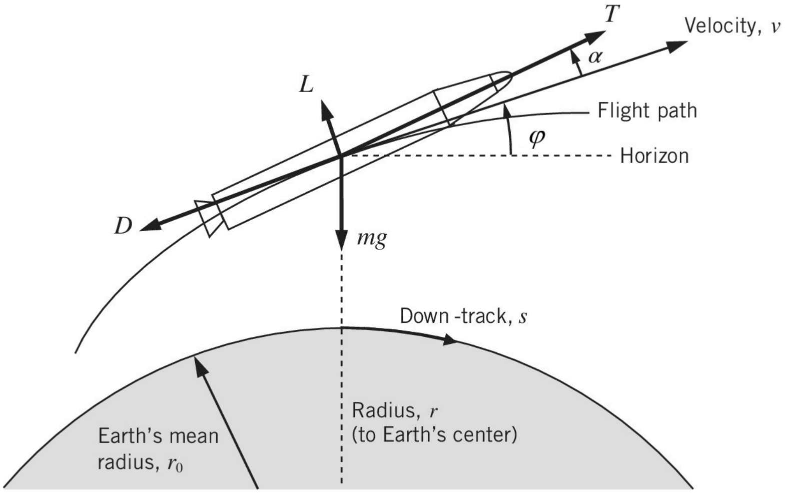
T
Velocity, v
α
L
Flight path
φ
Horizon
D
mg
Down -track, s
Earth's mean radius, r_0
Radius, r (to Earth's center)

Figure 3.1: Forces affecting the vehicle's motion [7]

1. losses due to misalignment: with T not parallel to v ($\alpha \neq 0$)

$$\int_{t_0}^{t_f} \frac{T}{m}(1-\cos\alpha)\,dt \tag{3.15}$$

2. aerodynamic losses: are air density, velocity and force dependent ($D = \rho \frac{{v_{rel}}^2}{2} S\, C_D$) , proportional to the square of the velocity and absent outside the atmosphere

$$\int_{t_0}^{t_f} \frac{D}{m}\,dt \tag{3.16}$$

3. gravity losses: are related to the fact that maneuvering in a gravitational field, part of the thrust, in case of flight path angle $\phi \neq 0$, is "eaten" by gravity with consequent losses

$$\int_{t_0}^{t_f} g\,\sin(\phi)\,dt \tag{3.17}$$

In outline, we could say:

$$\Delta v_{real} = \Delta v_{real} - \Delta v_{misalignment} - \Delta v_{drag} - \Delta v_{gravity}$$

That is:

$$v_f - v_i = \int_{t_0}^{t_f} \frac{T}{m}\, dt - \int_{t_0}^{t_f} \frac{T}{m} \left(1 - \cos\alpha\right) dt - \int_{t_0}^{t_f} \frac{D}{m}\, dt - \int_{t_0}^{t_f} g\, \sin\left(\phi\right) dt \tag{3.18}$$

3.2 Electric propulsion maneuvers

For the study of maneuvers with electric propulsion, the hypothesis of impulsive maneuvering lapses since the latter is characterized by low accelerations and small thrusts.
In order to describe realistically the maneuvers, it is therefore necessary to take into account the Edelbaum approximation, valid in the following hypotheses [8]:

1. almost-circular orbit:

$$r \approx a \approx p; \quad e \approx 0; \quad v^2 \approx \frac{\mu}{r}; \quad E \approx \nu \approx M.$$

2. low-inclination orbit:

$$\sin i \approx i; \qquad \cos i \approx 1,$$

   As reference plane we choose that of the initial orbit.

3. very-low thrust/acceleration (along $\vec{v}$, that is tangential):

$$\frac{T}{m} << \frac{\mu}{r^2}.$$

Assumptions 1 and 2 being valid, we introduce the alternative orbital parameter *true longitude* $l = \Omega + \omega + \nu$.
Given the above hypotheses, we can affirm therefore that, in the electric propulsion case, there is a gradual change in velocity that causes the spacecraft to follow a spiral trajectory.

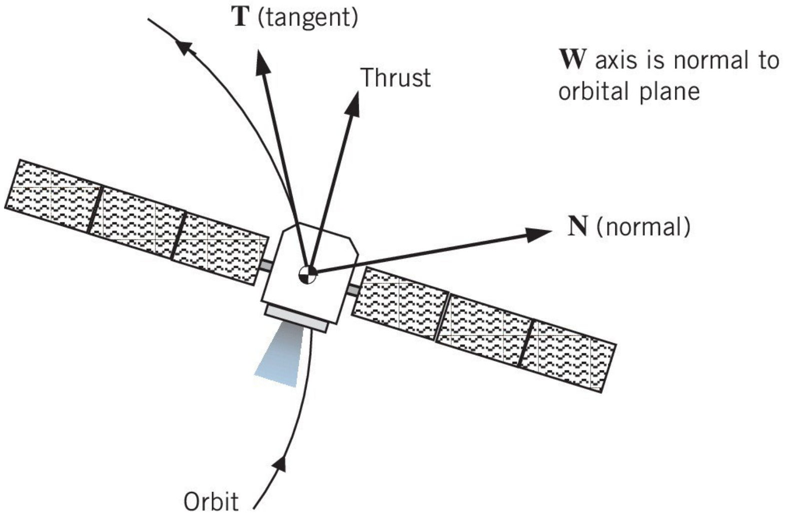

Figure 3.2: Thrust and its components ($N \equiv R$) [7]

The Gauss planetary equation, which describes the temporal variations of the orbital parameters, are simplified and become:

$$v\frac{da}{dt} = 2rA_T \tag{3.19a}$$

$$v\frac{de}{dt} = 2\cos\nu A_T + \sin\nu A_R \tag{3.19b}$$

$$v\frac{di}{dt} = \cos(\omega+\nu)A_W \tag{3.19c}$$

$$e\,v\,\frac{d\omega}{dt} = -e\,v\frac{d\Omega}{dt} + 2\sin\nu A_T - \cos\nu A_R \tag{3.19d}$$

$$i\,v\,\frac{d\Omega}{dt} = \sin(\omega+\nu)A_W \tag{3.19e}$$

$$\frac{dl}{dt} = \sqrt{\frac{\mu}{a^3}} \tag{3.19f}$$

Where A_T , A_R, and A_W represent respectively the tangential, the radial (outward), and the out-of-plane accelerations and are equal to the ratio of the thrust in that direction to the mass of the spacecraft.
From the equations in simplified form (3.19) we obtain therefore that:

- Thrusts in the tangential direction modify the energy so change a, e, ω
- Thrusts in the radial direction modify e, ω.
  It does not change the energy as it pushes perpendicular to $\vec{v}$, which does not change in modulus

- Thrusts perpendicular to the orbital plane modify i, Ω.
  The thrust component perpendicular to the orbital plane modifies the parameters that define the orientation of the plane in space.

However, some equations 3.19 present a singularity for $e, i = 0$, in fact $\dot{\omega}$ and $\dot{\Omega}$ tend to ∞; this is due to the fact that periastrum and ascending node are, in the case of circular and zero inclination orbits, undefined.
Edelbaum solved this problem by ignoring the equations that contained this singularity (eq. 3.19d and 3.19e). *Edelbaum equations* are therefore:

$$v\frac{da}{dt} = 2rA_T \tag{3.20a}$$

$$v\frac{de}{dt} = 2\cos\nu A_T + \sin\nu A_R \tag{3.20b}$$

$$v\frac{di}{dt} = \cos(\omega + \nu)A_W \tag{3.20c}$$

Starting from equations 3.20 the problem Edelbaum dealt with was to understand in which direction it is convenient to apply the thrust so as to optimize the variation of a, e, and i. The optimal direction of acceleration is determined by the particular objective that is to be achieved.
Since T/m is the modulus of acceleration, α the angle in the plane between the velocity vector $\vec{v}$ and the thrust vector $\vec{T}$, and β the angle between $\vec{T}$ and the plane of the orbit, we can express the acceleration components as it follows:

$$\begin{cases} A_T = \dfrac{T}{m}\cos\alpha\cos\beta \\[2ex] A_R = \dfrac{T}{m}\sin\alpha\cos\beta \\[2ex] A_W = \dfrac{T}{m}\sin\beta \end{cases} \tag{3.21}$$

From this, Edelbaum primarily addressed three issues:

Variation of the semi-major axis a

To obtain the maximum increase in a, it is necessary to apply the thrust in the tangential direction, therefore:

$$\alpha = \beta = 0 => A_T = A => \begin{cases} A_T = A \\ A_R = A_W = 0 \end{cases}$$

Applying thrust continuously for one full revolution results in a zero change in eccentricity while the change in inclination is zero at every point along the trajectory:

$$\Delta e = \Delta i = 0$$

Variation of the eccentricity e

For eccentricity-only variations, the optimal solution is obtained for:

$$\beta = 0$$

$$\tan\alpha = \frac{1}{2}\tan\nu$$

The equation defining the angle α is well approximated if we assume valid the law $\alpha = \nu$. From this approximation it results that the maximum variation of eccentricity is obtained by applying the thrust in a direction almost perpendicular to the line of apsides.
In this case the variations of semi-axis and inclination are zero in a complete turn:

$$\Delta a = \Delta i = 0$$

Combined variation of the semi-major axis a and of the inclination i

For combined variations of semi-axis and inclination the optimal solution is for:

$$\alpha = 0$$

$$\tan\beta = k\cos(\omega + \nu)$$

$$A_T = A\cos\beta \qquad A_R = 0 \qquad A_W = A\sin\beta$$

where k is a constant dependent on Δa and Δi and β is to be specified.
Also in this case there is an approximate solution that well follows the behavior of the exact one. This is possible by assuming that β takes on a constant value, $\bar{\beta}$, whose sign changes according to the sign of $\cos(\omega + \nu)$:

$$\begin{cases} \bar{\beta} > 0 & \text{if } \cos(\omega + \nu) > 0 \\ \bar{\beta} < 0 & \text{if } \cos(\omega + \nu) < 0 \end{cases}$$

In the case of multi-turn maneuvers there can be substantial variations of the orbital parameters, so at each revolution it is appropriate to redefine the β value. Solving the problem of β optimization, assuming almost circular trajectories with constant β during each revolution, we obtain:

$$\frac{\sin\beta}{\sqrt{r}} = \text{const}$$

From this, it can be seen that the plane change is more convenient at high radii, where the velocity is lower.

3.2.1 Coplanar Circle-to-Circle Transfer

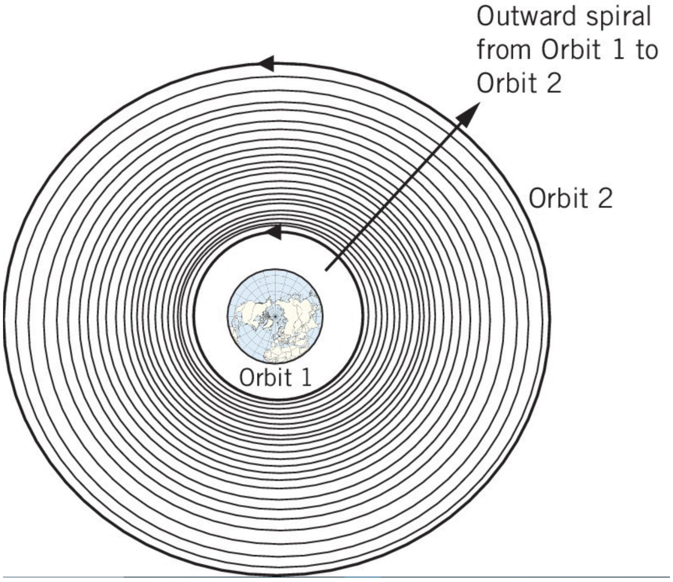

Figure 3.3: Coplanar Circle-to-Circle Transfer [7]

In the case of electric propulsion we have seen how, starting from the Edelbaum equations, to obtain an optimal variation of the orbital parameter a the assumptions listed in 3.2.
In terms of Δv we therefore obtain [9]:

$$\Delta v = \left| \sqrt{\frac{\mu}{a_0}} - \sqrt{\frac{\mu}{a_1}} \right| = |v_0 - v_1| \tag{3.22}$$

Where, since the orbits considered are circular orbits, the semi-major axis of the starting orbit $a_0 \equiv r_0$ and the semi-major axis of the final orbit $a_1 \equiv r_1$, so the Δv is a difference between circular velocities.

3.2.2 Inclination-Change Maneuver

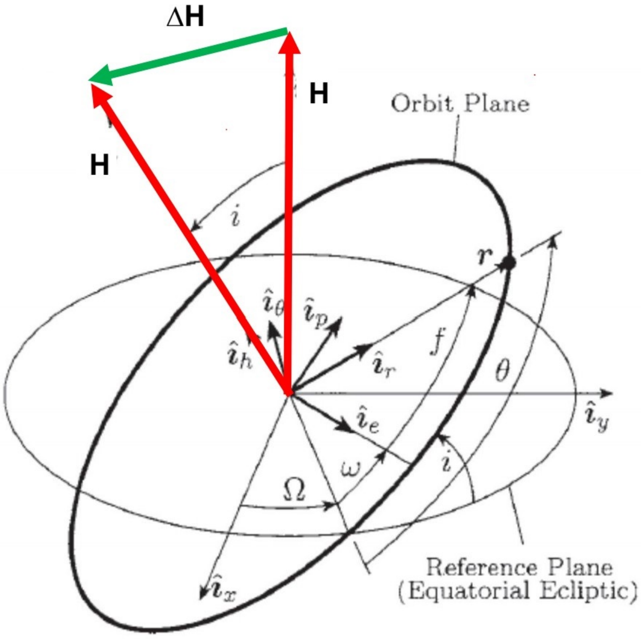
ΔH
H
H
Orbit Plane
i
r
$\hat{\imath}_\theta$
$\hat{\imath}_p$
$\hat{\imath}_h$
$\hat{\imath}_r$
f
θ
$\hat{\imath}_e$
$\hat{\imath}_y$
ω
i
Ω
Reference Plane
(Equatorial Ecliptic)
$\hat{\imath}_x$

Figure 3.4: Inclination Change [10]

In order to modify the inclination of the orbital plane it is necessary to push perpendicularly to it. As in the previous case, starting from Edelbaum equations it is possible to identify an optimal "pushing mode" and therefore a certain Δv, however it should be noted that the maneuver to modify the orbital parameter i is a particularly delicate maneuver, in this case it is necessary to change the direction of the angular momentum vector $\vec{H}$ without changing its magnitude. The main problem in case of tilt change with low thrust propulsion is when to push upwards and when to push downwards.
In terms of Δv we have two formulas that lead to almost similar results.
The first one is [9]:

$$\Delta v = v_0 \sqrt{2 - 2\cos\frac{\pi}{2}\Delta i} \tag{3.23}$$

The second option is [7]:

$$\Delta v = \frac{\Delta i \pi v_0}{2} \tag{3.24}$$

Where v_0 is the initial velocity and Δi represents the desired inclination change.

3.2.3 Transfer Between Inclined Circular Orbits

In sections 3.2.1 and 3.2.2, we proposed simple analytical expressions for two scenarios: a coplanar circle-to-circle transfer and an inclination change maneuver. Decoupling the changes in the orbital elements allowed us to solve the Gauss variational equations using variable separation and analytical integration. In 1961, T. N. Edelbaum obtained a closed-form solution for the general three-dimensional low-thrust transfer between inclined circular orbits. Edelbaum used optimization theory and the calculus of variations to develop the minimum propellant transfer between circular orbits with plane change.
In terms of Δv we have:

$$\Delta v = \sqrt{{v_0}^2 + {v_1}^2 - 2v_0 v_1 \cos\frac{\Delta i \pi}{2}} \tag{3.25}$$

3.2.4 Walking

In the case of rendezvous maneuvers with low thrust propulsion we typically speak of *walking* [11].
It is possible to obtain a generally valid result that is suitable for both impulsive maneuvers, for which we have already provided formulas in section 2.2.4, and for low thrust maneuvers. Call $\Delta\theta$ the angular distance we want to cover with the maneuver,the general approach is to transfer to a lower (for $\Delta\theta > 0$) or higher (for $\Delta\theta < 0$) nearby orbit, then drift in this faster (or slower) orbit for a certain time, then return to the initial orbit. The analysis is similar for high and low thrust, because in either case the spacecraft is nearly in the same orbit even during thrusting periods, and as we found out for spiral transfers, the Δv for orbit transfer is equal to 3.22.

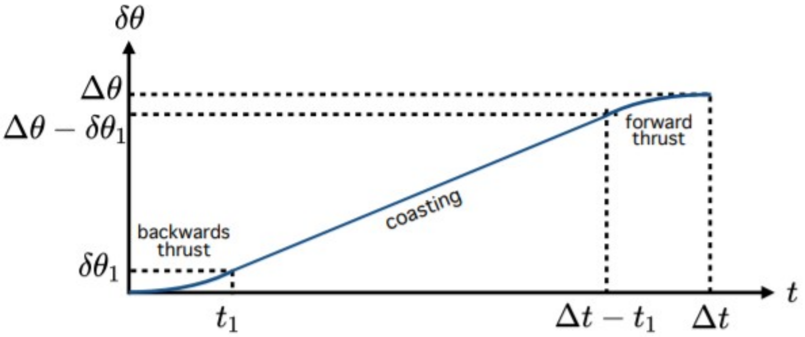

Figure 3.5: General shape of the Walking maneuver. $\delta\theta$ is the advance angle relative to a hypothetical satellite remaining in the original orbit and left undisturbed. [11]

For the low-thrust case, continuous thrusting is used during both legs.
It can be shown that the Δv for the maneuver is equal to [11]:

$$\Delta v = \frac{4}{3}\,\frac{r_0\,\Delta\theta}{(\Delta t + t_c)} \tag{3.26}$$

where r_0 is the radius of the beginning circular orbit and t_c is the *coasting time*.

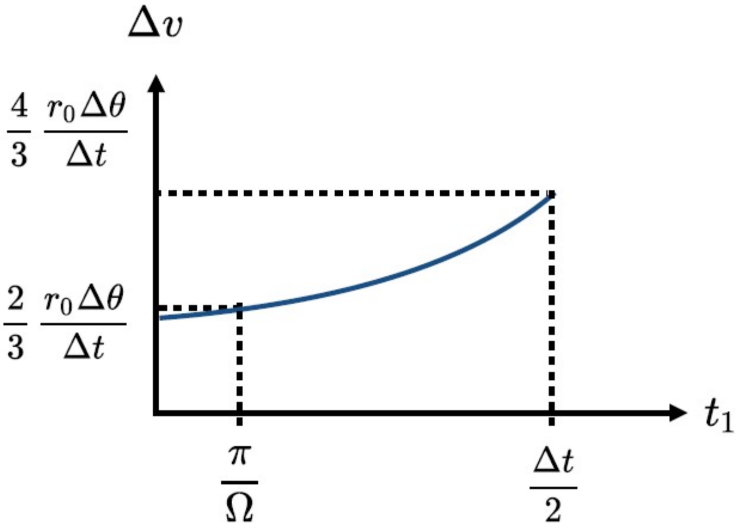

Figure 3.6: Δv for the Walking maneuver [11].

3.3 Electric Thrusters

In the case of electric propulsion, the energy source is separate from the propellant and does not depend on it, therefore a power generator is needed.
The main energy sources exploited and/or planned for electric propulsion are:

- **solar panels**: provide electrical power directly;
- **radioisotope energy**: requires the conversion of heat into electrical energy;
- **nuclear fission reactors**: require energy conversion.

Fixed the generator and established its power is possible to modify c or I_{sp} by varying the thrust or flow rate that we want to obtain. Therefore an additional parameter is available, the *electrical power* P_E. P_E and $\dot{m}_p$ (3.2) are two independent parameters; I_{sp} can grow arbitrarily by:

- reducing the propellant flow rate $\dot{m}_p$ (the available power is fixed);

- increasing the electrical power P_E.

It is therefore clear that the available energy is independent of the energy needed to accelerate the propellant.
With electric propulsion it is possible to obtain higher I_{sp} than with chemical propulsion, however a power generator is required which involves additional weight and which must be taken into account in the overall cost calculation.

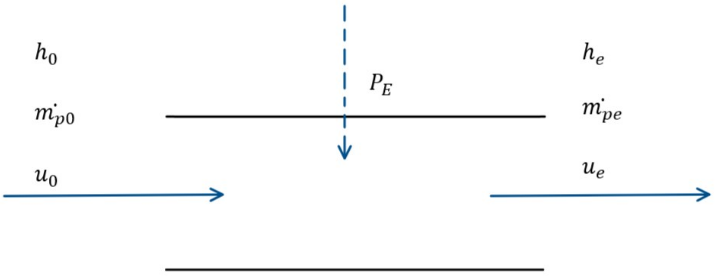

Figure 3.7: Scheme for application of first principle to electric propulsion (subscript 0 means input, subscript e means exit).

As can be seen from the schematic in Figure 3.7, we supply electrical power P_E to the propellant mass $\dot{m}_p$, which is converted into kinetic energy of the gas:

$$\dot{m}_p\left(h_e + \frac{u_e^2}{2} - h_0\right) = \eta P_E \tag{3.27}$$

Assuming the input velocity to be nearly zero. Since $u_e \simeq c$, from eq.3.4 it follows that:

$$P_T = \eta P_E \tag{3.28}$$

Where η is the overall efficiency (often significantly smaller than 1).
From eq. 3.4 and 3.28 we obtain:

$$c = \sqrt{2\eta \frac{P_E}{\dot{m}_p}} \tag{3.29}$$

Since eq. 3.3 is always valid we have:

$$c = \frac{2\eta P_E}{T} \tag{3.30}$$

So from eq. 3.29 and 3.30 it follows that to modify c and I_{sp} we can manage, as already said, P_E and $\dot{m}_p$. The acceleration that can be obtained with electric propulsion is limited compared to chemical propulsion, the thrust times are therefore

very long. This characteristic influences, as we have seen, the trajectory to follow; to make some displacements many orbit turns will be necessary, in each of which there will be a small variation. On the other hand, when using electric propulsion each mission will be characterized by an optimal value of specific impulse.
Both of these effects are related to the weight of the generator.

Some useful relationships between the characteristic masses of the S/C are introduced below.
The initial spacecraft mass is:

$$m_0 = m_u + m_p + m_s \tag{3.31}$$

Where m_u is the *payload mass*, m_p is the *propellant mass* and m_s is the *power source mass*. The generic mass at a given time instant t, m, will therefore be:

$$m = m_u + m_p + m_s \geq m_s \tag{3.32}$$

The power source mass penalize the payload which is reduced by m_s:

$$m_u = m_0 - m_p - m_s \tag{3.33}$$

We can assume that the power source mass is proportional to the electrical power by a coefficient α, known as *specific power generator mass*:

$$m_s = \alpha P_E = \frac{\alpha}{\eta}\frac{Tc}{2} \tag{3.34}$$

The ratio $\dfrac{\alpha}{\eta} = \beta$ defines a sort of *technological level* the will be useful to perform the mission analysis for electric propulsion.

Types of electric propulsion

A first broad subdivision of electric propulsion can be as follows:

- **Electrothermal**: gas is heated by electrical energy and expands in a nozzle;
- **Electrostatic**: the propellant is accelerated by electrostatic forces;
- **Electromagnetic**: the propellant is accelerated by electromagnetic forces.

The following provides some generalities of the types of thrusters that were considered in chapter 4.

3.3.1 Hall Effect Thrusters

Hall thrusters are electrostatic ion accelerators in which the grid system is replaced by a relatively strong magnetic field perpendicular to the flow. This magnetic field prevents backflow of electrons into the accelerating field and, as will be shown, eliminates the space charge limitation that restricts the flow and thrust of ion engines (Child's law) [12].

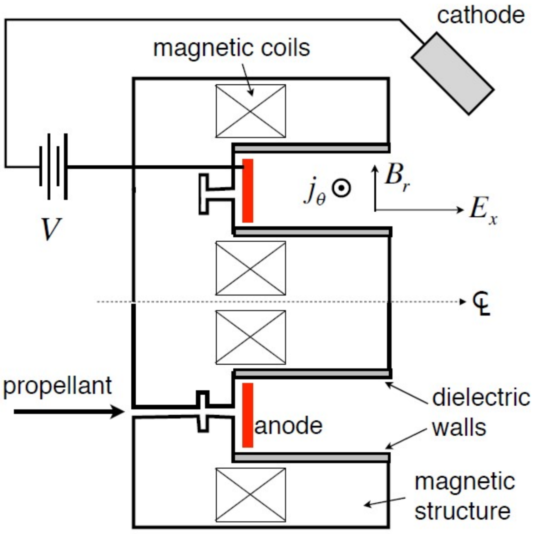

Figure 3.8: Schematic of an Hall Effect Thruster [12]

A schematic of an Hall Effect Thruster (HET) is shown in Figure 3.8. From the longitudinal section, the axisymmetric geometry of a typical HET can be observed. It basically consists of an annular cavity coaxial to the inner cylinder in which plasma is created by the passage of current between the annular anode, located at the bottom of a cavity made of dielectric material (chamber), and the externally positioned cathode. Once the plasma is created, a radial magnetic field is applied, either via ring-shaped permanent magnets, or via soft iron coils and yokes.The magnetic field slows down considerably the average axial velocity of electrons, which, due to the low collision rate (in HETs we have in fact $\Omega_{Hall} >> 1 \iff$ high Hall parameter $\iff$ few collisions), are forced to perform mainly collisions with electrons. they are forced to perform mainly drifts in the direction of $\vec{E} \times \vec{B}$, i.e., around the ring, while being radially confined by sheaths on the insulating walls. The ions meanwhile, are only weakly affected by the magnetic field $\vec{B}$ and, if the density is low enough and thus collisions are rare, they are simply accelerated by the electrostatic field to a velocity u_+:

$$u_+ = \sqrt{2\,\frac{q}{m_+}\,V} \tag{3.35}$$

The name "Hall Thruster" is derived from the mechanism by which thrust forces are exerted on the solid parts of the motor. As indicated, the ions are simply accelerated by the electrostatic field, but since the ions are in a nearly neutral plasma, an equal and opposite electrostatic force is exerted on the free electrons in that plasma.

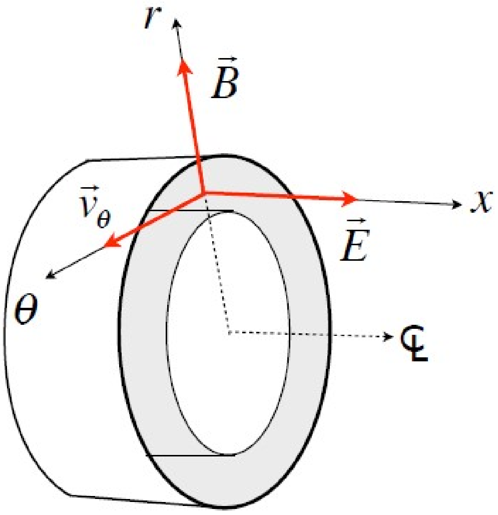

Figure 3.9: Hall Effect in an HET [12]

However, in the presence of the radial magnetic field, these electrons are not free to accelerate toward the anode; instead, they move in the azimuthal direction (perpendicular to $\vec{E}\times\vec{B}$) at such a velocity that they generate an equal and opposite magnetic force on themselves. If we denote the forward axial direction by x, the electrons end up drifting with a velocity v_θ known as *drift velocity*:

$$v_\theta = \frac{\vec{E}\times\vec{B}}{B^2} \tag{3.36}$$

The ions have no such azimuthal drift (their *Larmor radius* is larger than the device's length), and so a net azimuthal current density arises, called a *Hall current*:

$$j_\theta = -qn_e\frac{\vec{E}\times\vec{B}}{B^2} \tag{3.37}$$

Where n_e is the number of the electrons. Given this current, the magnetic (Lorentz) force density on it is $\vec{f} = \vec{j_\theta} \times \vec{B}$; an equal and opposite force is exerted by the plasma currents on the Hall Effect thruster. It follows that:

$$\vec{f} = qn_e\vec{E} \tag{3.38}$$

The important point is that the structure is not electrostatically acted on (electric fields and electric pressures in this case are too weak), but magnetically, through the Hall current - hence the name.

Table 3.1: Hall Effect - Ion Thrusters Comparison

Type	Hall	Ion
Propellant	Xe	Xe
I_{sp} [sec]	1500-2500	2000-4000
P_E [W]	300-6000	200-5000
η	0.5	0.65
Voltage [V]	200-600	1000-2000
Thruster mass [kg/kW]	2-3	3-6
PPU mass [kg/kW]	6-10	6-10
Feed System	Regulated	Regulated
lifetime [h]	>7000	>10000
missions	med-ΔV	large-ΔV

3.3.2 Enhanced Magnetic Plasma Thrusters

In this subsection we give some background on the working principle of an Enhanced Magnetic Plasma Thruster (EMPT), this is a cathode-free RF thruster specifically designed for CubeSat propulsion and developed at Technology for Propulsion and Innovation S.r.l. (T4i) in collaboration with the Center for Space Studies and Activities (CISAS) of the University of Padua.[13]

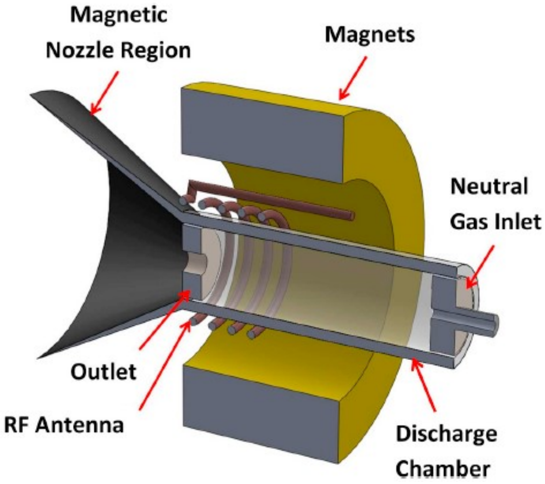

Figure 3.10: Enhanced Magnetic Plasma Thruster [13]

The main design drivers, which made the realization of the MET very challenging, are miniaturization, low power consumption, and the achievement of good propulsive performance (i.e., thrust from 300 N to 900 N and specific impulse up to 900 s). To illustrate the operating principle of a cathode-free thruster, it is worthwhile to briefly address the phenomena governing plasma dynamics inside the discharge chamber and in the magnetic nozzle. The key physical phenomena governing plasma dynamics in the discharge chamber are EM wave propagation, plasma transport, and their mutual coupling. The magnetic nozzle region extends downstream of the plasma source. Here the plasma is accelerated and eventually detaches from the magnetostatic field lines. The magnetic nozzle region is characterized by the formation of a plume where the plasma is more rarefied than in the source. Two regions, called near and far, respectively, can be discriminated within the plume depending on the phenomena governing the plasma dynamics. In the near region, particle collisions and the geometry of the applied magnetostatic field drive the behavior of the plasma. In contrast, in the far region, plasma expansion is governed primarily by thermal pressure and ambipolar diffusion.

3.3.3 Microwave Electrothermal thrusters

In the field of electrothermal thrusters it is possible to define, in addition to the most known and widespread categories of resistojets and arc jets, the so-called Microwave Electrothermal Thrusters (MET).
The operating modes of arc jets and resistojets have in fact soon showed some limitations of no small importance: resistojets have the technological limitation related to the maximum temperature of the resistance; arc jets, however, have

the technological limitation related to the maximum temperature of the electrodes (which, in addition, are subject to erosion). These limitations are inevitably reflected in limits on the achievable I_{sp}.

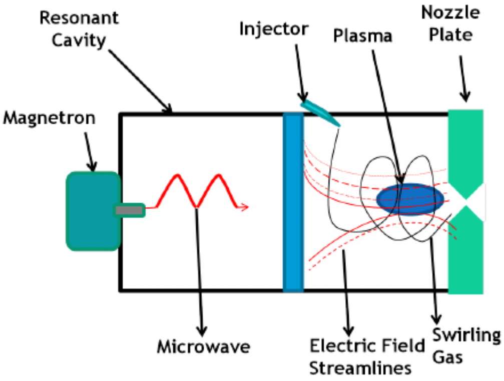

Figure 3.11: Microwave Electrothermal Thruster Schematic

In order to overcome these limitations METs have been introduced. Below we briefly summarize the operating principle of METs; the peculiarity of these thrusters is that the discharge is generated in the absence of electrodes, this mode of generation of the discharge, however, requires the generation of electromagnetic radiation through microwaves, in order to make up for the lack of electrons of the cathode. The EM waves therefore deposit energy in the fluid and, therefore heat the propellant. More in detail,The physical process of conversion of microwave energy into heat in the MET is threefold.

1. The microwave electric field accelerates electrons to higher energy, and these electrons then collide with atoms and molecules in the dense gas-plasma mixture.

2. The electrons thus transfer energy to the electronic and vibration-rotation modes of the molecules and atoms, which then

3. convert this into thermal energy by colliding with each other inelastically. Energy thus thermalizes and becomes equipartitioned.

Therefore, the energy flow is from the microwave fields, to the free electrons in the plasma, to the bound electron modes of the atoms and molecules that the free electrons collide with, and finally to thermal motion of the atoms and molecules through intermolecular inelastic collisions. This process is very efficient and leads to 99% microwave absorption by the plasma.The plasma thus soaks up energy as fast it is delivered into the cavity [14]. Di seguito elenchiamo rapidamente caratteristiche rilevanti dei METs:

- typical frequency: $\omega = 10^{10} Hz$;
- energy is directly absorbed by free electrons ($\omega_{\mu waves} < \omega_{e-plasma}$); the electrons accelerate, collide and heat the ionized gas;
- necessary layer of cold gas to protect the walls;
- thermal efficiency issues

Chapter 4

Mission Analysis for electric propulsion

In chemical propulsion we tend to choose the combination of propellants that provides the highest I_{sp}, maximizing the payload by decreasing the propellant on board. As already mentioned above the case of electric propulsion is quite different since increasing the I_{sp} means increasing the weight of the power generator (m_s); we can however see how, in this case, there is a value of *optimal* I_{sp}, unique for each mission, able to maximize the payload mass m_u and therefore the value of the ratio $\frac{m_u}{m_0}$. We should note that increasing the I_{sp} increases m_u but decreases the mass of propellant m_p required to perform the mission, on the other hand it should be noted that the engine that in this analysis we are going to assimilate to the power source, has its own weight not negligible, while the payload, despite increasing with the I_{sp}, at some point will stop growing. For these reasons it is therefore possible, as mentioned above, to search for an optimal point.
To perform this study we impose a set of simplifying assumptions:

- the initial mass m_0 is assigned
- the efficiency η and the specific power generator mass α are independent of c (and hence of I_{sp}).

Since we are interested in identifying the I_{sp} for a mission characterized by electric propulsion only, in the following we will propose the treatment for primary propulsion (in case of auxiliary propulsion the upstream assumptions basically change and therefore what is reported later is not valid).

Mission-Strategy-Technological Level

As part of this analysis we will assume that three control parameters are known, viz:

1. *Mission* i.e. the ΔV
2. *Strategy* that is the available thrust T
3. *Technological Level* i.e. the ratio $\dfrac{\alpha}{\eta} = \beta$

To express the link between I_{sp} and payload m_u we resort to some of the relations introduced in the chapter 3, readjusting them in the manner most suitable for this discussion. Since the relation 3.14 is valid and, having expressed m_s as 3.34 from which

$$\frac{m_s}{m_0} = \alpha \frac{P_E}{m_0} = \frac{\alpha}{\eta} \frac{Tc}{m_0\, 2} = \beta \, \frac{Tc}{m_0\, 2} \tag{4.1}$$

we already have 2 interesting relations in which the three introduced control parameters appear. We can also define a relation to explicate $\dfrac{m_p}{m_0}$ which, being m_p at the end of the mission equal to $m_0 - m_f$, results expressible as:

$$\frac{m_p}{m_0} = 1 - \frac{m_f}{m_0} = 1 - \exp\left(- \frac{\Delta v}{c} \right) \tag{4.2}$$

Instead, the payload m_u can be expressed, since it is equal to $m_0 - m_p - m_s$, as:

$$\frac{m_u}{m_0} = \exp\left(- \frac{\Delta v}{c} \right) - \frac{\alpha}{\eta} \frac{Tc}{2\, m_0} = \exp\left(- \frac{\Delta v}{c} \right) - \frac{\beta}{2} \frac{T\, c}{m_0} \tag{4.3}$$

Already from this expression we can see how the generator mass m_s subtracts payload.
Just the payload fraction m_u/m_0 is the quantity we are interested in optimizing in relation to the specific impulse. Starting from the last expression in 4.3, where all the control parameters appear, we can search for an optimal value by setting the first derivative of 4.3 equal to 0:

$$\frac{d}{dc}\left(\frac{m_u}{m_0} \right) = \frac{\Delta v}{c^2} \exp\left(\frac{-\Delta v}{c} \right) - \frac{\beta}{2} \frac{T}{m_0} = 0 \tag{4.4}$$

From the equation 4.4 we therefore derive an expression for c:

$$c = \sqrt{\frac{2\, m_0\, \Delta v \exp\left(- \dfrac{\Delta v}{c} \right)}{\beta\, T}} \tag{4.5}$$

From eq. 4.5 we can by iterative method find the c and thus the I_{sp} of optimum:

```
c_ciclo = DeltaV;
err = 1;
while err > 10^(-6)          % error > tollerance
    c_new = sqrt((2*m_0*DeltaV*exp(-DeltaV./c_ciclo))./(Beta*T));
    err = abs(c_new - c_ciclo);
    c_ciclo = c_new;
end
```

Where the last c_{new} into the loop is the optimal one, c_{opt}.

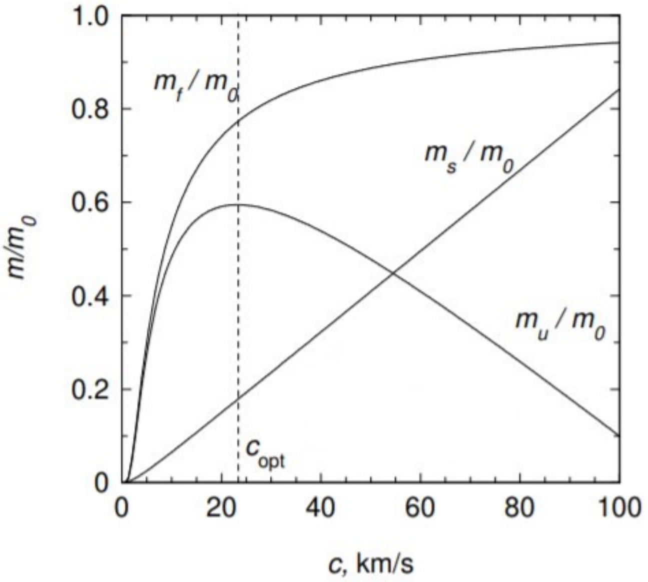

Figure 4.1: c_{opt} example [8]

What we expected from this formulation is that as β (higher efficiency) decreases and as push T decreases, fixed the other parameters, there is a growth in the value of c_{opt}.

Mission-Time-Technological Level

A similar analysis can be conducted by considering instead of the *strategy*,i.e. the Thrust parameter T, an alternative parameter, namely the time to complete the mission, that we will rename *Time* Δt. So in this case the three control parameters are:

1. *Mission* i.e. the ΔV
2. *Time* that is the available time for the mission Δt
3. *Technological Level* i.e. the ratio $\dfrac{\alpha}{\eta} = \beta$

Since thrust is no longer a control parameter, the expressions previously identified for mass fraction are no longer usable. It is therefore necessary to identify relations that are dependent only on Δv, Δt, β.
Basically what we will do for this analysis is to replace the Thrust T with the Δt. For the mass fraction $\dfrac{m_f}{m_0}$ and $\dfrac{m_p}{m_0}$ the expressions 3.14 and 4.2 remain valid, as they continue to exploit control parameters known to us. What changes is the expression of $\dfrac{m_s}{m_0}$, for which we can no longer use the expression containing the thrust. Since T is defined as equation 3.3, expressing the propellant flow rate $\dot{m}_p$ as:

$$\dot{m}_p = \frac{m_p}{\Delta t} \tag{4.6}$$

We can write by using 4.2 and 4.6:

$$\frac{m_s}{m_0} = \frac{\beta}{2}\frac{T\,c}{m_0} = \frac{\beta}{2}\frac{c^2}{\Delta t}\frac{m_p}{m_0} = \frac{\beta}{2}\frac{c^2}{\Delta t}\left(1 - \exp\left(-\frac{\Delta v}{c}\right)\right) \tag{4.7}$$

Also the expression of $\dfrac{m_u}{m_0}$ changes:

$$\frac{m_u}{m_0} = 1 - \frac{m_p}{m_0} - \frac{m_s}{m_0} = \exp\left(-\frac{\Delta v}{c}\right) - \frac{\beta}{2}\frac{c^2}{\Delta t}\left(1 - \exp\left(-\frac{\Delta v}{c}\right)\right) \tag{4.8}$$

Similarly to the previous case, starting from the last expression in 4.8, where all the control parameters appear, we can search for an optimal value by setting the first derivative of 4.8 equal to 0:

$$\frac{d}{dc}\left(\frac{m_u}{m_0}\right) = 0$$

Where $\dfrac{d}{dc}\left(\dfrac{m_u}{m_0}\right)$ is:

$$\frac{d}{dc}\left(\frac{m_u}{m_0}\right) = \frac{\Delta v}{c^2}\exp\left(-\frac{\Delta v}{c}\right) - \frac{\beta}{2\Delta t}\left[2c\left(1 - \exp\left(-\frac{\Delta v}{c}\right)\right) - \Delta v\exp\left(-\frac{\Delta v}{c}\right)\right] \tag{4.9}$$

By performing the appropriate steps we can obtain an expression for the effective discharge velocity c:

$$c = \frac{\Delta t \, \exp\left(-\frac{\Delta v}{c}\right)}{\beta}\left(\frac{\Delta v}{c^2}+\frac{\beta\Delta v}{2\,\Delta t}+\frac{\beta c}{\Delta t}\right) \tag{4.10}$$

The expression 4.10, certainly more complex than the previous one 4.5, is suitable for dealing with the problem with the data at our disposal $(\Delta v, \Delta t, \beta)$. Also in this case, from eq. 4.10 we can by iterative method find the c and thus the I_{sp} of optimum, assigned the available mission time:

```
c_ciclo_time = DV_time;
err = 1;
while err > 10^(-6)      % error > tollerance
    c_new2 = Dt_time*exp(-DV_time/c_ciclo_time)/Beta_time*...
        ((DV_time/c_ciclo_time^2)+(Beta_time*DV_time/(2*Dt_time))+...
        (Beta_time*c_ciclo_time/Dt_time));
    err = abs(c_new2 - c_ciclo_time);
    c_ciclo_time = c_new2;
end
```

4.1 Preliminary Analysis

In order to carry out the mission analysis for electric propulsion effectively, it was necessary to define and/or hypothesize in advance all the control parameters previously listed. To this purpose, we have decided to divide this paragraph into four sub-sections in order to be able to evaluate all the factors considered.
Before going into these aspects, it is necessary to define some characteristics of the mission and of the IOSHEXA motorized dispenser. To this end, the following is the Concept of Operations of the IOSHEXA mission, which also provides some technical specifications that have been studied in a parallel thesis work carried out at SAB (M. Guerzoni 2021).

1. Integration and Test Operations:

Table 4.1: Integration and Test Operations

	Integration and Test Operations
Project integration and test:	Test and Integration with #3 12U cubesat deployers and #1 robotic system for debris capture in SAB Aerospace s.r.o. facility in Brno (CZ). Overall Mass of the IOSHEXA System 700 kg.
Launch Integration:	Final integration and pre-flight operations are performed in the European Space Port in French Guiana

2. Launch Operations:

Table 4.2: Launch Operations

	Launch Operations
Ascent:	Ascent Phase using the VEGA launch vehicle. This phase will be managed by ARIANESPACE from the European Space Port in French Guiana.
Deployment:	The IOSHEXA S/C is released by AVUM on an SSO orbit at 550 km with an initial velocity and attitude. After the release the commissioning phase starts to achieve full system calibration
Early Orbit Phase:	Early Orbit Phase is used to perform a verification that all systems are healthy in order to prepare the S/C for operations. Commissioning is completed in this phase.

3. Technological Demonstrator Operations:

Table 4.3: Technological Demonstrator Operations

	Technological Demonstrator Operations
Operative Orbit:	Now the IOSHEXA S/C is fully active and healthy and on a stable AVUM's orbit. IOSHEXA starts its transfer towards customers requested orbits for cubesat deployment.
Debris Orbit:	After all cubesats needs have been cleared, the transfer towards the debris orbit can start. We want to reach an 823 km height, SSO ($\Delta i \simeq 1$ deg).
Phasing:	In order to approach the debris IOSHEXA starts phasing maneuvers (Phasing Angle = 90 deg)
SAFIR approach:	Rendezvous, proximity maneuvers and capture of the debris are performed.

4. End of Life:

Table 4.4: End of Life

	End of Life
Delayed Deorbit:	Disposal operations occur at the end of project life. These operations are used to either provide a controlled reentry of the S/C. The IOSHEXA performs an orbit lowering.
Atmospheric Reentry:	Once the satellite reaches the "delayed deorbit" orbit, it remains in low orbit for a period of time less than 25 years (as imposed by the regulations)

4.1.1 Mission: Δv

We define below, in more detail, the type of mission that we want to achieve, with particular regard to what are the propulsive costs understood as Δv.

As mentioned in the introductory chapter and in the previous section, the one proposed in this thesis work is an IOD mission voluntarily aimed exclusively at electric propulsion. So we have to evaluate the best propulsive solution for a Low Thrust mission in LEO.

The two reference orbits are presented in the figure:

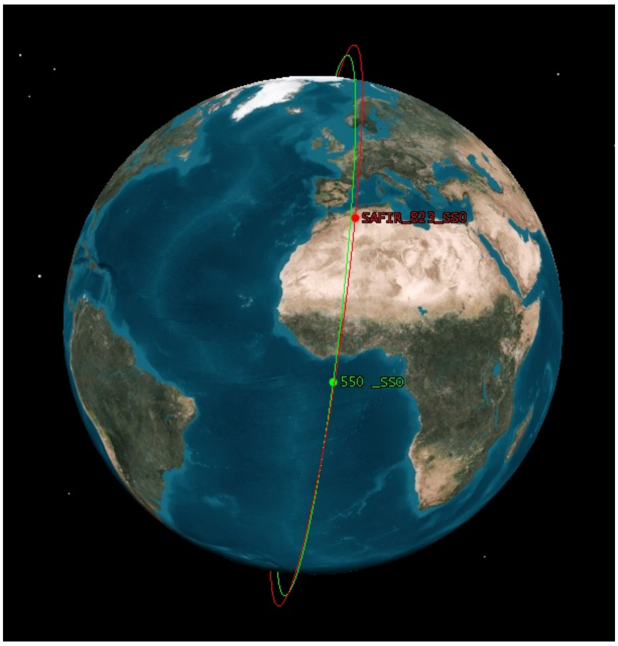

Figure 4.2: Reference Orbit of the IOD mission

The calculations for the evaluation of the Δv of the mission were carried out using matlab and verified with the help of a software developed by AGI, System Tool Kit (STK). The maneuvers analyzed are reported below and exploit formulas already introduced in the previous chapter.
The constants and parameters considered to perform the calculations are reported here:

```
% Earth Gravitational Constant [km^3/sec^2]:
mi = 398600;
% Earth Radius [km]:
Rp = 6371;
% Orbit Height Considered [km]:
z = [550,823];
% Orbit inclinations [deg]:
incl = [97.59251383, 98.8];
% semi-major axis (orbit radius if circular orbit) [km]:
r = Rp+z;
% Total Specific Mechanical Energy of the Orbits [km^2/sec^2]:
Eg = -mi./(2*r);
Eg1 = Eg(1);
Eg2 = Eg(2);
% Circular Velocity [km/sec]:
v_c = sqrt(mi./r);
V_c1 = v_c(1);              %Circular velocity z = 550km
V_c2 = v_c(2);              %Circular velocity z = 823km
```

- *Periaps Raising*: IOSHEXA has been released by AVUM on a sun-synchronous orbit at an altitude of 550 km, this one has been selected because of the strong requests from all the cubesat producers for the insertion in SSO. Here the space-tug performs the release of satellites that need to be placed in this orbit acting as a simple dispenser on which are placed the cubesat deployers. Once these operations are completed, the possibility of maneuvering comes into operation. It is assumed that the remaining unreleased satellites need to be placed on an SSO at higher altitude (823 km):

```
    % DeltaV spiral [m/sec]:
    DV_spiral = abs(V_c1-V_c2)*1000;
```

$$\Delta v_{spiral} = 145.3873\,[m/s]$$

- *Simple plane change*: as anticipated, it is assumed that in addition to the increase in altitude, the clients satellites need to remain on an SSO, therefore it is also necessary to change the inclination $\Delta i \simeq 1.2\,[deg]$; the change of inclination could take place either at 550 km or 823 km altitude, therefore both results are reported:

```
 % DeltaVs simple plane change [m/sec]:
 for i = 1:length(v_c)
 Di = incl(2)-incl(1);
 Di = deg2rad(Di);
 DV_simpl_LowThrust(i) = v_c(i)*sqrt(2-2*cos(pi*Di/2))*1000;
 end
```

$$\Delta v_{Plane\,550} = 251.214\,[m/s]$$

$$\Delta v_{Plane\,823} = 246.401\,[m/s]$$

In general it is observed that the plan change maneuver is more efficient when performed in the orbit characterized by lower speed (specific mechanical energy in absolute value is reduced)

- *Transfer Between Inclined Circular Orbits*: an alternative solution that, in the hypothesized scenario, appears better, could be the combined maneuver. The propulsive cost of a maneuver able to raise the altitude of the starting circular orbit and at the same time to change its inclination has been evaluated as follows:

```
 % DeltaV Combined Maneuver [m/sec]:
 DV_combined_LowThrust = sqrt(V_c1^2+V_c2^2-2*V_c1*V_c2*cos(Di
*pi/2))*1000;
```

$$\Delta v_{Combined\,Maneuver} = 288.1613\,[m/s]$$

- *Phasing*: it is assumed that once on the 823km SSO, the system would need to reposition itself at an angle due to, for example, a request from customers who need to have a certain angular offset. Such a maneuver can also be assumed as a simulation, although extremely simpler, of a SAFIR debris approach maneuver, towards which the SAB LS will turn in the development of the next missions, its attention. The propulsive cost of the phasing maneuver (often the term *walking* is also used as mentioned above) is:

```
 % DeltaV Walking [m/sec]:
 DV_walking = 4/3*(r(2)*pi)/((24*60*60))*1000;
```

$$\Delta v_{Walking} = 348.775\,[m/s]$$

- *Delayed Deorbit*: we suppose in this case to lower the satellite to an altitude of 300 km so that the aerodynamic actions of the atmosphere can then intervene causing the decay of the satellite:

```
    % Deorbit's orbit radius [km]
    r_deorbit = Rp+H_deorbit;
    % Circular velocity deorbit is orbit [km/sec]
    v_c_deorb = sqrt(mi/r_deorbit);
    % DeltaV De-orbit [m/sec]:
    DV_deorb_electric = abs(v_c_deorb-V_c2)*1000;
```

$$\Delta v_{deorbit} = 286.2807\,[m/s]$$

Since the in-orbit timescales are in any case less than one year in duration (although not specified at this stage of the study) it was deemed unnecessary to directly evaluate the costs in terms of Δv for station keeping.

Table 4.5: Δv resume

	Maneuver	$\Delta v\,[m/s]$	Δv with ESA Margins $[m/s]$
	1) Periaps Raising	145.387	159.926
	2) Simple plane change (a)	251.214	276.335
	3) Simple plane change (b)	246.401	271.041
	4) Combined Maneuver	288.161	316.977
	5) Phasing	348.775	383.653
	6) Delayed Deorbit	286.281	314.909
$\Delta v_{tot} - 1$	Solution 1: 2)+1)+5)+6)	1031.700	1134.900
$\Delta v_{tot} - 2$	Solution 2: 1)+3)+5)+6)	1026.800	1129.500
$\Delta v_{tot} - 3$	**Solution 3**: 4)+5)+6)	**923.217**	**1015.500**

Solution 3 being the least onerous, it was chosen to proceed with the mission analysis.

4.1.2 Strategy: *T*

The strategy parameter described here refers to the thrust capabilities that will characterize the ideal thruster for the considered mission.
In order to define this parameter, it has been chosen to consider the thrusters that have been studied among the most suitable engines from worldwide companies

to evaluate which of them is closest to an ideal solution. IIt is therefore clear that the engines considered will be characterized by performances that are not optimized for the mission, while the mission analysis aims precisely at identifying the characteristics of an engine tailored to the mission itself; for this reason, it was decided to take as input only the thrust values supplied and then make the necessary evaluations through a trade-off on the propulsion.
There are a total of five thrusters that could be considered, belonging to the categories described in the subsections 3.3.1, 3.3.2, 3.3.3 and reported here:

Hall Effect Thruster:

- HT400: HET produced by the Italian company SITAEL. The HT 400 Hall Effect Thruster (HET) has been designed to perform orbit and attitude control tasks on micro and mini satellites. Its design, based on permanent magnets, is conceived to be installed onboard of Telecommunication and Earth observation platforms. In particular, it is in the forefront of Low Power Hall Effect Thrusters (LP-HET), thruster class especially suitable for small satellites where power and mass budgets are strongly limited [15].
- PPS X00: HET produced by the French company Safran. While the PPS 5000 and PPS 1350 thrusters cater to high- and medium-power needs, there is also a growing need for low-power thrusters, which will be used for satellite constellations in particular. With a view to offering a product to this market segment, Safran worked alongside the CNES to initiate the development of a new electric thruster, the PPS X00, from 270 to 1,000 W of power [16].
- ExoMG micro: HET produced by the French company Exotrail. Exotrail claims to be able with its technology to dramatically reduce the size of HETs while ensuring minimal mission and system impact. Due to the relatively high thrusts, it is possible to drastically reduce mission duration [17].

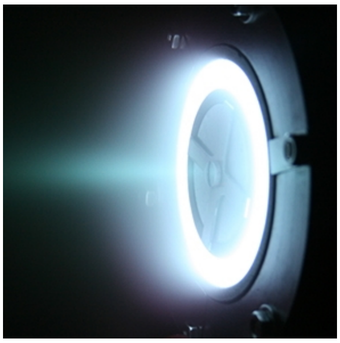

Figure 4.3: ExoMG - micro in operation [17]

Ehnanced Magnetic Plasma Thruster:

- REGULUS-based: EMPT produced by the Italian company T4innovation. This engine, not already available, will be based on the existing REGULUS, a propulsion platform for CubeSats. It integrates the Magnetically Enhanced Thruster, and its subsystems (i.e., fluidic line, electronics, and thermo-structural components)[13].

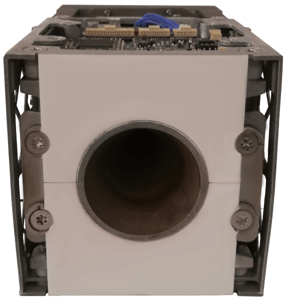

Figure 4.4: REGULUS [18]

Microwave Electrothermal Thruster:

- AQUAMET: MET produced by the URA, an AVS space spin-off born in 2019. This MET create a free-floating plasma discharge in a cylindrical cavity resonator, efficiently heating a wide range of propellants while providing high thrust to power ratio. The water-fuelled AQUAMET also features high specific impulse, from a simple, robust thruster at low cost [19].

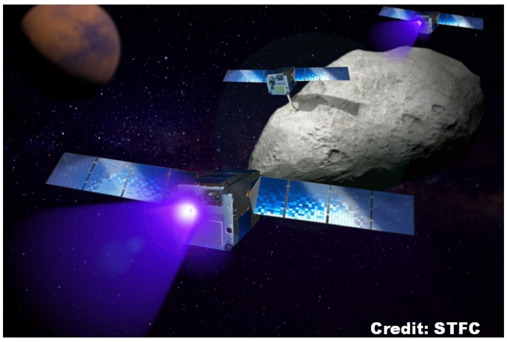

Credit: STFC

Figure 4.5: AQUAMET [19]

The table summarizes the main characteristics collected, with particular reference to the thrust values that will be taken as reference in the mission analysis. The cluster option is present if proposed by the manufacturer.

Table 4.6: Thrusters specific [20],[21] (* esteem)

Thruster	# of thrusters (cluster if $\neq$ 1)	Total Propulsion System Mass* [kg]	I_{sp} $[sec]$	Power $[W]$	Thrust $[N]$
REGULUS based	1	125.18	500	500	0.005
AQUAMET	2	85	800*	1000*	0.200*
exoMG micro	4	76	1000*	800*	0.040*
HT400	1	45	1529	800	0.040
PPS X00	1	43	1650	1000	0.075

4.1.3 Technological Level: β

The third parameter we are going to consider is the technology level β. This parameter is defined by the ratio between α, specific mass of the power generator [kg/W], and β, propulsive efficiency of the power generator, for this reason it is difficult with the data at our disposal to determine a value of β common to each engine taken into account in the definition of the strategy (it is also dependent on the technological capabilities of manufacturers). In this work, therefore, we will limit ourselves to assume values of β that are compatible with the current average technological possibilities; for this reason we will avoid too small values of β, indicative of an extremely advanced technology and not yet in use in space (e.g. nuclear propulsion $\alpha = 1\,[kg/kW]$).

β values considered:

- $\beta_1 = 50\,[kg/kW]$
- $\beta_2 = 25\,[kg/kW]$

4.1.4 Time: Δt

The last parameter to consider is the time available to complete the mission to be designed. This parameter is an alternative to the *strategy* parameter and allows to obtain the characteristics of an ideal "tailor-made" engine. Since the IOSHEXA payload is exclusively technological and the mission in question is a demonstration mission, the timing, in this case, is not to be considered as such a stringent parameter. On the other hand, it should be noted that the service provided by

IOSHEXA is, in addition to ADR and future In-Orbit Servicing applications, also a "shuttle" service for small satellites, therefore customer requirements are certainly a variable that must be taken into account. At the input of the company supervisor, two timeframes have been taken into consideration:

Δt values considered:

- $\Delta t_1 = 30\, days$
- $\Delta t_2 = 45\, days$

4.2 Mission analysis IOSHEXA

Taking into account that the total mass of the system is 700 kg as described in tab.4.1, we report the results for the following cases:

- cases #a: Mission-Strategy-Technology - with variable thrust and $\beta = 50$
- cases #b: Mission-Strategy-Technology - with variable thrust and $\beta = 25$
- cases #c: Mission-Time-Technology - with variable Time and $\beta = 50$
- cases #d: Mission-Time-Technology - with variable Time and $\beta = 25$

Case 1a

Table 4.7: Input for case 1a

$\Delta v\,[m/s]$	$T\,[mN]$ (REGULUS based)	$\beta\,[kg/kW]$
1015.5	5	50

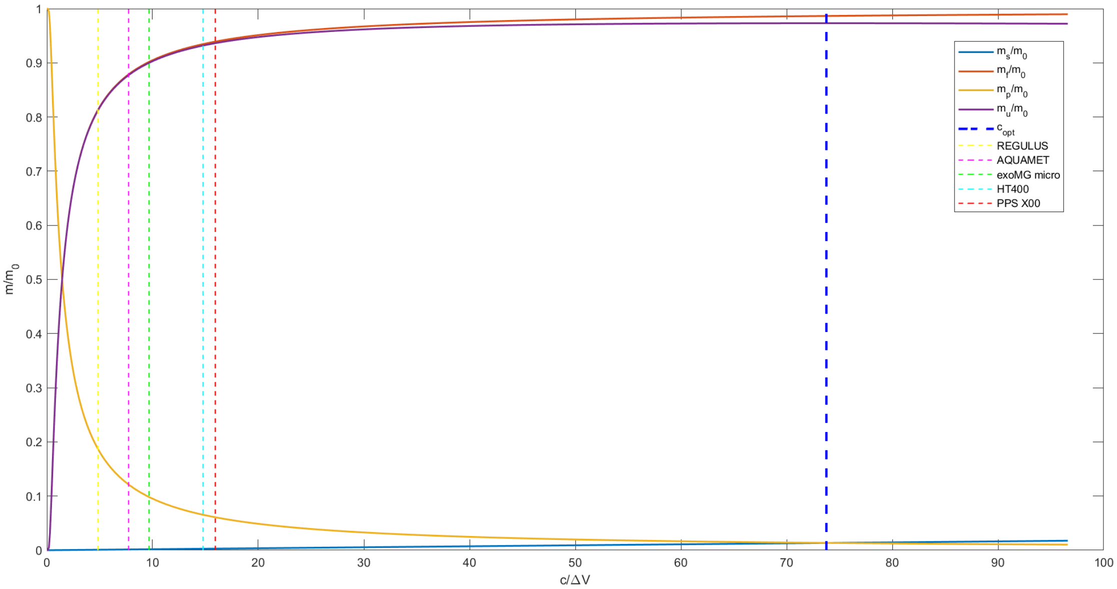

Figure 4.6: Optimal I_{sp} for case 1a

Table 4.8: Output for case 1a

	Optimal I_{sp} results
Optimal I_{sp} [sec]	7635.2
Final Mass m_f [kg]	690.5736
Power Source Mass m_s [kg]	9.3627
Propellant Mass m_p [kg]	9.4264
Payload Mass m_u [kg]	681.2109
Mission Duration t [days]	1634.4
Thrust Power P_T [W]	187.2535

Case 2a

Table 4.9: Input for case 2a

$\Delta v\,[m/s]$	$T\,[mN]$ (AQUAMET)	$\beta\,[kg/kW]$
1015.5	200	50

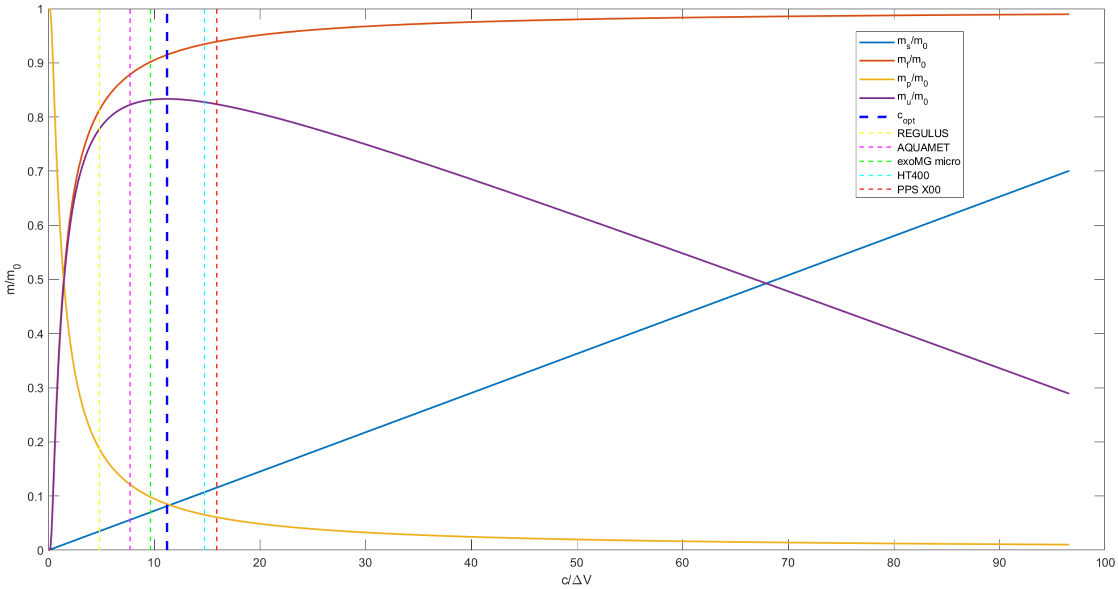

Figure 4.7: Optimal I_{sp} for case 2a

Table 4.10: Output for case 2a

	Optimal I_{sp} results
Optimal I_{sp} [sec]	1162.5
Final Mass m_f [kg]	640.3628
Power Source Mass m_s [kg]	57.0214
Propellant Mass m_p [kg]	59.6372
Payload Mass m_u [kg]	583.3414
Mission Duration t [days]	39.3588
Thrust Power P_T [W]	1140.4

Case 3a

Table 4.11: Input for case 3a

$\Delta v\,[m/s]$	$T\,[mN]$ (exoMG micro) (HT400)	$\beta\,[kg/kW]$
1015.5	40	50

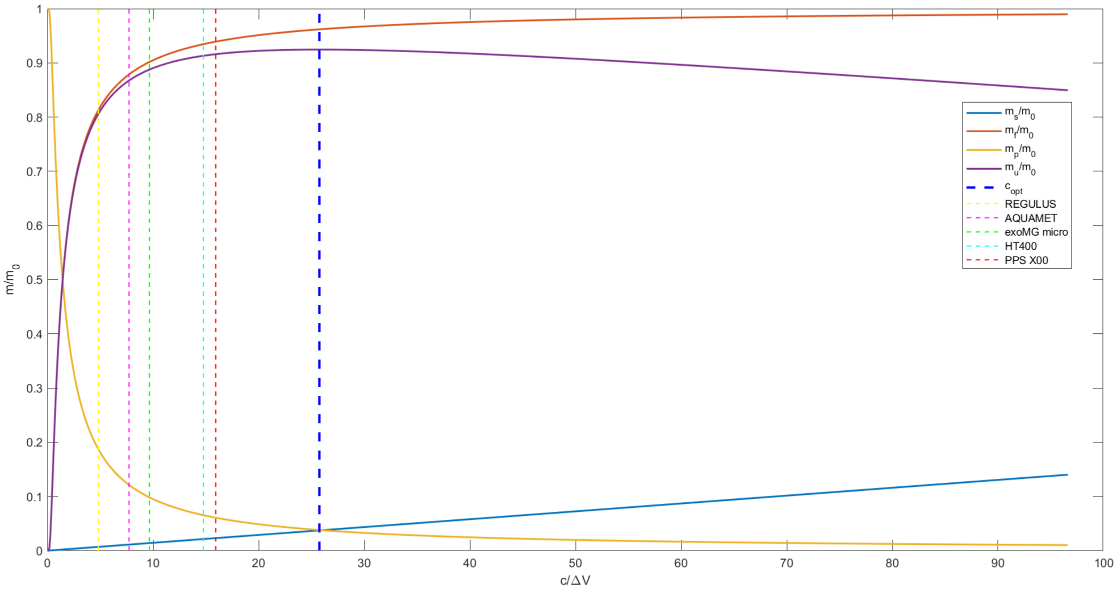

Figure 4.8: Optimal I_{sp} for case 3a

Table 4.12: Output for case 3a

	Optimal I_{sp} results
Optimal I_{sp} [sec]	2665.6
Final Mass m_f [kg]	673.3366
Power Source Mass m_s [kg]	26.1491
Propellant Mass m_p [kg]	26.6634
Payload Mass m_u [kg]	647.187
Mission Duration t [days]	201.7431
Thrust Power P_T [W]	522.9812

Case 4a

Table 4.13: Input for case 4a

$\Delta v\,[m/s]$	$T\,[mN]$ (PPS X00)	$\beta\,[kg/kW]$
1015.5	75	50

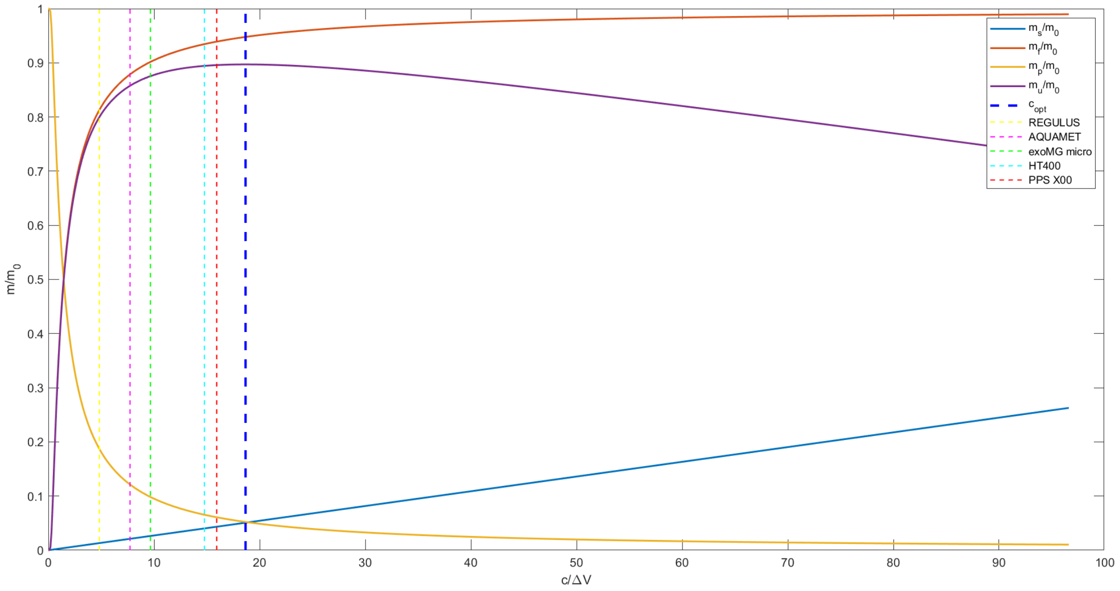

Figure 4.9: Optimal I_{sp} for case 4a

Table 4.14: Output for case 4a

	Optimal I_{sp} results
Optimal I_{sp} [sec]	1932.4
Final Mass m_f [kg]	663.4875
Power Source Mass m_s [kg]	35.5432
Propellant Mass m_p [kg]	36.5125
Payload Mass m_u [kg]	627.9443
Mission Duration t [days]	106.8125
Thrust Power P_T [W]	710.8647

Case 1b

Table 4.15: Input for case 1b

$\Delta v\,[m/s]$	$T\,[mN]$ (REGULUS based)	$\beta\,[kg/kW]$
1015.5	5	25

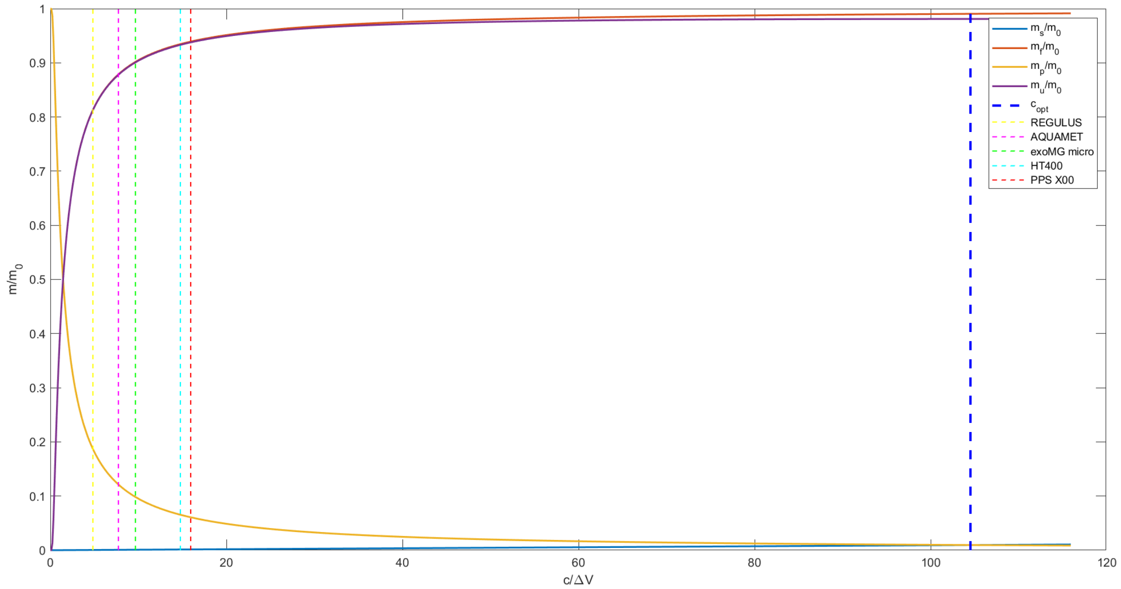

Figure 4.10: Optimal I_{sp} for case 1b

Table 4.16: Output for case 1b

	Optimal I_{sp} results
Optimal I_{sp} [sec]	10819
Final Mass m_f [kg]	693.3345
Power Source Mass m_s [kg]	6.6336
Propellant Mass m_p [kg]	6.6655
Payload Mass m_u [kg]	686.7089
Mission Duration t [days]	1637.6
Thrust Power P_T [W]	265.3453

Case 2b

Table 4.17: Input for case 2b

$\Delta v \, [m/s]$	$T \, [mN]$ (AQUAMET)	$\beta \, [kg/kW]$
1015.5	200	25

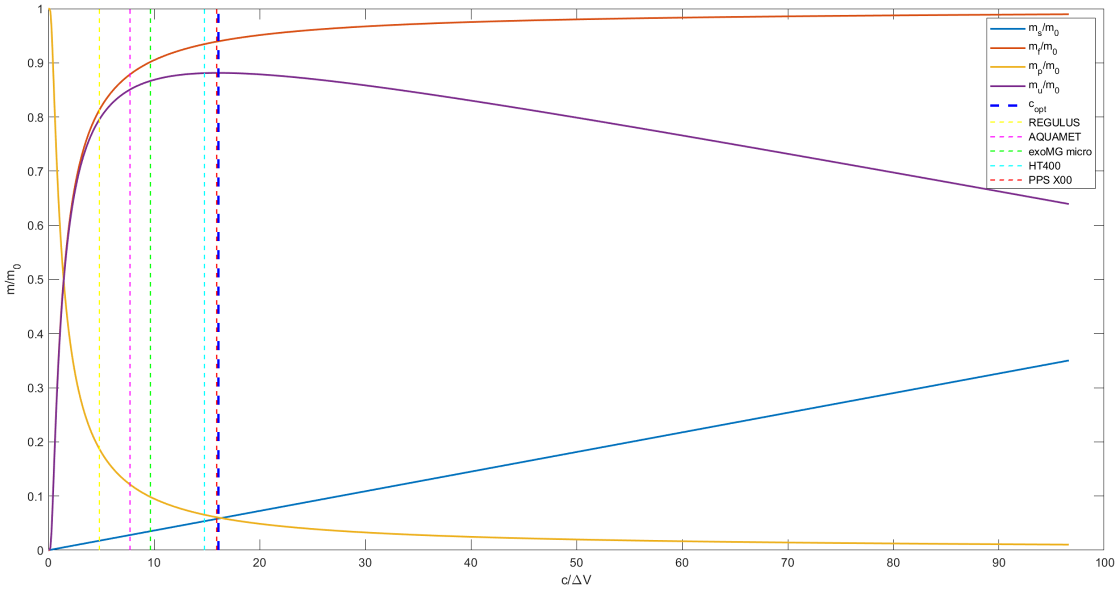

Figure 4.11: Optimal I_{sp} for case 2b

Table 4.18: Output for case 2b

	Optimal I_{sp} results
Optimal I_{sp} [sec]	1666.3
Final Mass m_f [kg]	657.8373
Power Source Mass m_s [kg]	40.8667
Propellant Mass m_p [kg]	42.1627
Payload Mass m_u [kg]	616.9706
Mission Duration t [days]	39.8854
Thrust Power P_T [W]	1634.7

Case 3b

Table 4.19: Input for case 3b

$\Delta v\,[m/s]$	$T\,[mN]$ (exoMG micro) (HT400)	$\beta\,[kg/kW]$
1015.5	40	25

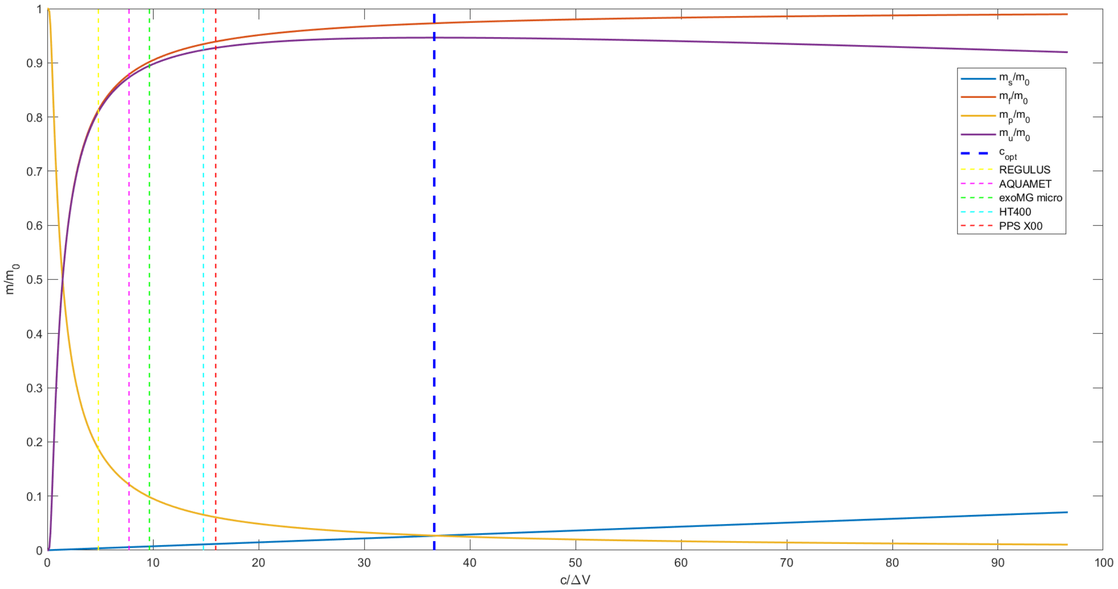

Figure 4.12: Optimal I_{sp} for case 3b

Table 4.20: Output for case 3b

	Optimal I_{sp} results
Optimal I_{sp} [sec]	3791.5
Final Mass m_f [kg]	681.1467
Power Source Mass m_s [kg]	18.5971
Propellant Mass m_p [kg]	18.8533
Payload Mass m_u [kg]	662.5496
Mission Duration t [days]	202.9033
Thrust Power P_T [W]	743.8841

Case 4b

Table 4.21: Input for case 4b

$\Delta v\,[m/s]$	$T\,[mN]$ (PPS X00)	$\beta\,[kg/kW]$
1015.5	75	25

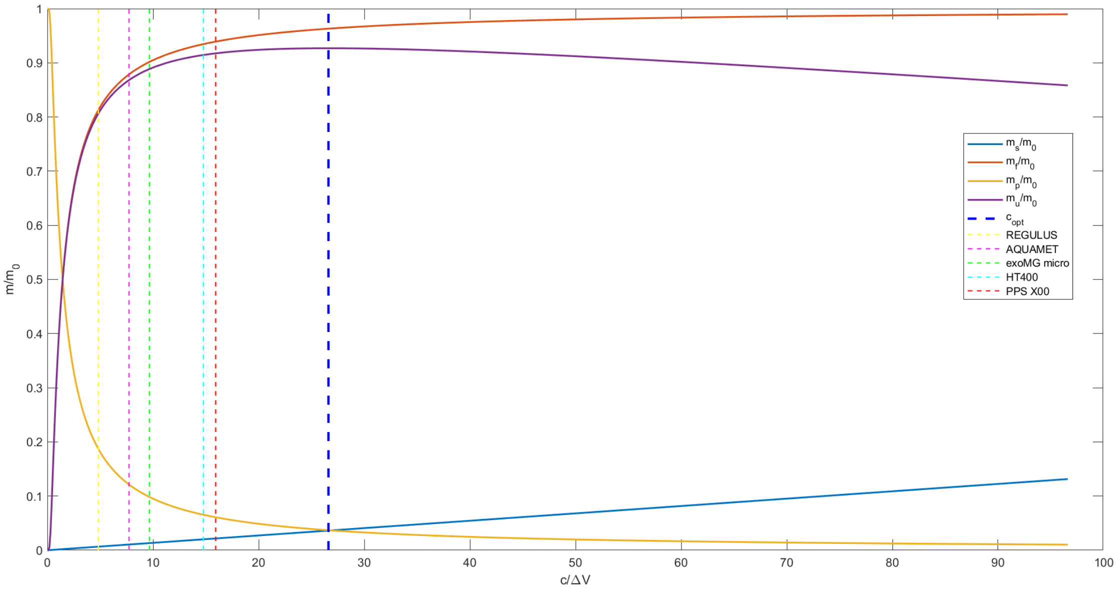

Figure 4.13: Optimal I_{sp} for case 4b

Table 4.22: Output for case 4b

	Optimal I_{sp} results
Optimal I_{sp} [sec]	2754.7
Final Mass m_f [kg]	674.1833
Power Source Mass m_s [kg]	25.3346
Propellant Mass m_p [kg]	25.8167
Payload Mass m_u [kg]	648.8487
Mission Duration t [days]	107.6635
Thrust Power P_T [W]	1013.4

Case 1c

Table 4.23: Input for case 1c

$\Delta v\,[m/s]$	$Time\,\Delta t\,[days]$	$\beta\,[kg/kW]$
1015.5	30	50

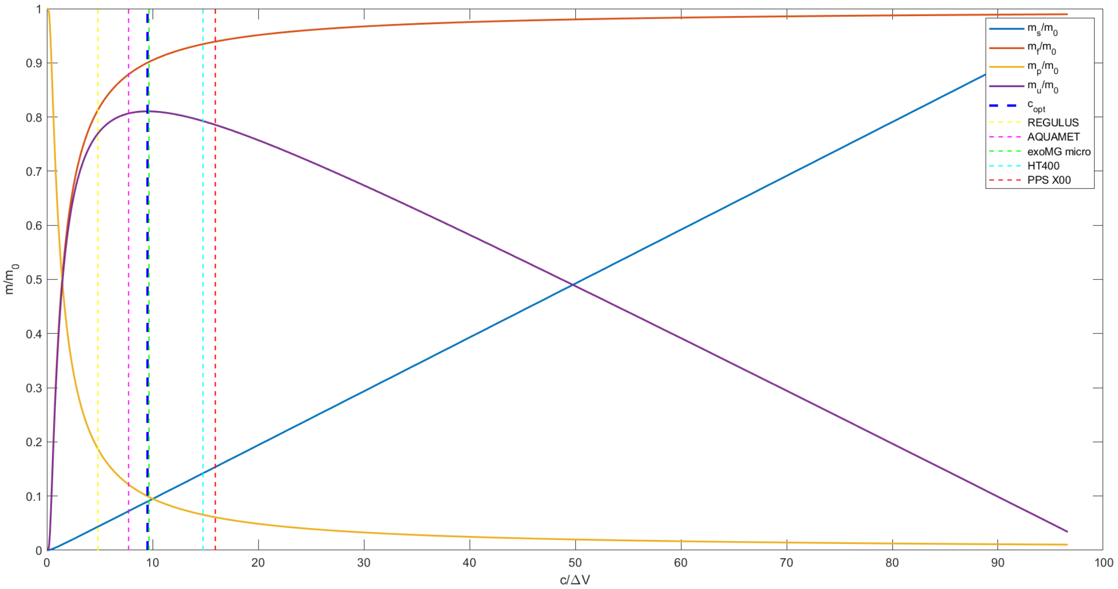

Figure 4.14: Optimal I_{sp} for case 1c

Table 4.24: Output for case 1c

	Optimal I_{sp} results
Optimal I_{sp} [sec]	985.7201
Final Mass m_f [kg]	630.2168
Power Source Mass m_s [kg]	62.9363
Propellant Mass m_p [kg]	69.7832
Payload Mass m_u [kg]	567.2805
Thrust T [N]	0.2603
Thrust Power P_T [W]	1258.7

Case 2c

Table 4.25: Input for case 2c

$\Delta v\,[m/s]$	$Time\,\Delta t\,[days]$	$\beta\,[kg/kW]$
1015.5	45	50

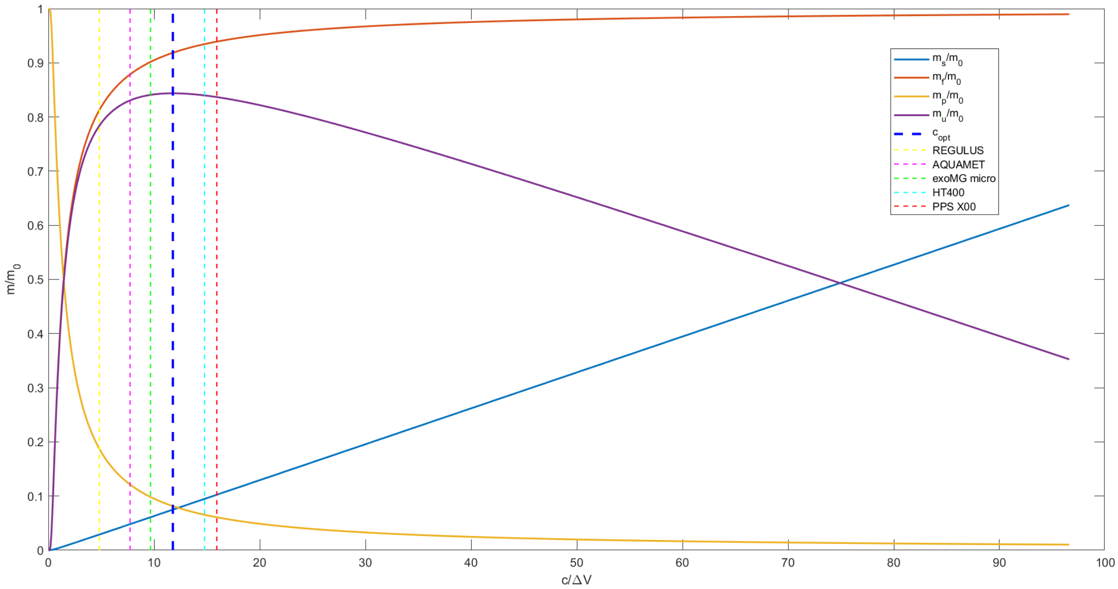

Figure 4.15: Optimal I_{sp} for case 2c

Table 4.26: Output for case 2c

	Optimal I_{sp} results
Optimal I_{sp} [sec]	1219.1
Final Mass m_f [kg]	643.0144
Power Source Mass m_s [kg]	52.4069
Propellant Mass m_p [kg]	56.9856
Payload Mass m_u [kg]	590.6075
Thrust T [N]	0.1753
Thrust Power P_T [W]	1048.1

Case 1d

Table 4.27: Input for case 1d

$\Delta v\,[m/s]$	$Time\,\Delta t\,[days]$	$\beta\,[kg/kW]$
1015.5	30	25

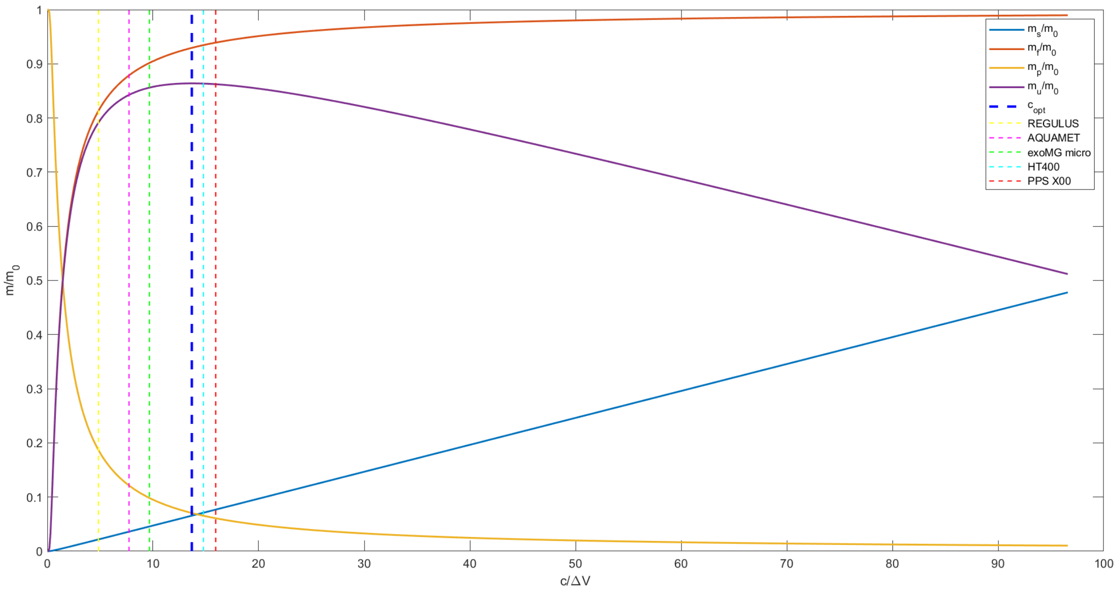

Figure 4.16: Optimal I_{sp} for case 1d

Table 4.28: Output for case 1d

	Optimal I_{sp} results
Optimal I_{sp} [sec]	1415.8
Final Mass m_f [kg]	650.6456
Power Source Mass m_s [kg]	45.9140
Propellant Mass m_p [kg]	49.3544
Payload Mass m_u [kg]	604.7316
Thrust T [N]	0.2645
Thrust Power P_T [W]	1836.6

Case 2d

Table 4.29: Input for case 2d

$\Delta v\,[m/s]$	$Time\,\Delta t\,[days]$	$\beta\,[kg/kW]$
1015.5	45	25

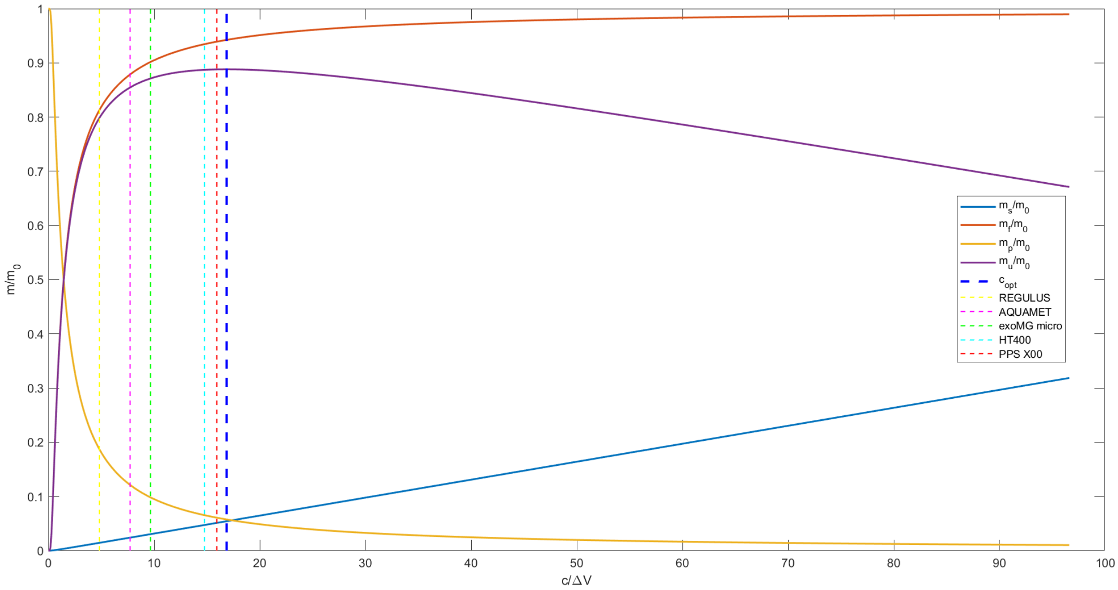

Figure 4.17: Optimal I_{sp} for case 2d

Table 4.30: Output for case 2d

	Optimal I_{sp} results
Optimal I_{sp} [sec]	1745.8
Final Mass m_f [kg]	659.6996
Power Source Mass m_s [kg]	38.0019
Propellant Mass m_p [kg]	40.3004
Payload Mass m_u [kg]	621.6977
Thrust T [N]	0.1775
Thrust Power P_T [W]	1520.1

4.2.1 Analysis of results

Taking into analysis the various cases proposed above, it is possible to make some interesting considerations. First of all it is possible to observe that, having performed a mission analysis for primary propulsion, the optimum is not reached in case of equal value of the mass fraction m_s/m_0 and m_p/m_0; in particular it is observed that m_p/m_0 is slightly larger than m_s/m_0. This peculiarity, is preserved in all cases and is a consequence of the fact that the propellant mass, in case of primary propulsion is consumed throughout the mission and, therefore, is a consumable mass that is lost as we go forward, while the mass of the thruster is preserved until the end of the mission. It is therefore clear that, in order to perform the mission more efficiently, it is convenient to have a smaller thruster mass even if you carry a little more propellant with you. Always in a general way, it can be observed that the final mass curve m_f/m_0 (Tsiolkovsky curve) remains unchanged when the control parameters are varied. Having made this general consideration, let's observe in more detail first of all the results of the analysis for the cases where the only parameter to vary is the "strategy" parameter, that is the thrust T. In this case, comparing the outputs for increasing values of thrust (from 5 to 200 mN), it is possible to highlight how, once the other parameters are fixed, the increase in thrust has a negative impact on the payload m_u that can be carried to destination, with an obvious increase in the mass of propellant m_p needed and the mass of the power source (generator) m_s. The need to push harder also clearly affects the $I_{sp_{opt}}$ which is reduced at increasing values of thrust. Positive are the reduction of the mission duration (we push much more to cover the same propulsive distance - Δv, and with the same technology) and the increase of the thrust power, both related to a more relevant thrust. If instead we vary the technology level β, comparing for example cases 2a and 2b, increasing the technology level and therefore reducing the beta value (we consider the technology more efficient), we have probably an increase in the value of c_{opt} or of $I_{sp_{opt}}$, with consequent increase, all other parameters being equal, of the thrust power $P_{T\,opt} = \frac{T\,c_{opt}}{2}$. Analytically, this occurs because as we increase the technology level, the Tsiolkowsky curve remains unchanged while the generator curve is lowered because we have a larger optimal specific impulse, a larger optimal effective discharge velocity, and thus we can have a smaller generator mass to perform the mission optimally. It follows that as the generator mass and propellant mass are reduced, the payload at our disposal, increases. However, a slight increase in the time required to perform the mission should be noted.

Moving on to analyze cases #c and #d, i.e., those that consider the mission duration as the control parameter instead of the thrust parameter, we can see how the results of the analysis vary.Ì Comparing two cases with the same Δv and Δt but different β, as the technology improves (β decreases), there corresponds an increase in the optimal specific impulse and thrust power (e.g. cases 1c to 1d). It is interesting to compare this result with a similar pair of cases from the previous analysis, conducted at the same Δv and T and reduction in β (e.g. cases 2a-2b). In that case it was observed that the improvement of the technology with the same thrust provided, resulted in a slight increase in the duration of the mission; in cases 2a and 2b instead, having constrained the duration, this choice affects the analysis with a slight increase in the thrust obtained. Finally, by varying the duration parameter, thus allowing the mission to take place over a longer period of time and with the other control parameters Δv and β being equal (e.g. cases 1c-2c), what is observed is an increase in the payload fraction, a reduction in the thrust T and a reduction in the thrust power.

4.2.2 Trade-Off Propulsion Systems

Following the market survey an analysis on data gathered started in order to evaluate the criteria on which the trade-off is based. Criteria chosen to be considered in this Phase 0 trade-off are: *Transfer Time* (see appendix B), *Thruster Mass* which is the total propulsion system mass (dry mass + propellant mass), and *Power Consumption.* These were chosen because they are factors with the most impact on final spacecraft mass and costs. Transfer time represents a cost: a long time to perform maneuvers means a long lifetime for the mission, that needs to be sustained with many resources. Thruster mass also influences the final mass. Mass and volume not only have a direct impact on the costs of the spacecraft and on the complexity of subsystems, but also have consequences on the launch capacity requested to the launcher provider to embark. Finally, Power Consumption is the input power needed and would determine the power production system design, with impacts on costs, volume, and mass of the final configuration.

In order to select the best propulsive solution, an Analytical Hierarchy Process (AHP) has been carried out on the basis of these parameters in order to identify which is the best compromise for the achievement of mission objectives.

By using a Prioritization Matrix, a normalized scale with values between 0 and 1 has been created; in that way, each parameter considered was therefore associated with a number to indicate its importance in relation to the mission carried out.

Table 4.31: AHP Propulsion Trade-off

Selection Criteria	Description	Weighting (Normalized Value)
Transfer Time	Takes into account the time required to transfer considering a given propulsion solution. The result in terms of weight in the AHP, takes into account the fact that no stringent time requirements were defined in this first analysis.	0.182
Thruster Mass	It takes into account what will be the overall mass of the propulsion system including the weight of the generator. We are interested in a solution that is as light as possible.	0.545
Power Consumption	It takes into account the power levels needed to operate the engine. The least power-intensive solution is preferred.	0.273

On the basis of these three selection criteria and the results obtained from these various cases considered for the mission analysis, we defined which of the five propulsion solutions considered could be considered the winning solution for potential application to the IOSHEXA mission. The excel-table below shows the results of the analysis and the PPS X00 is the most convenient solution.

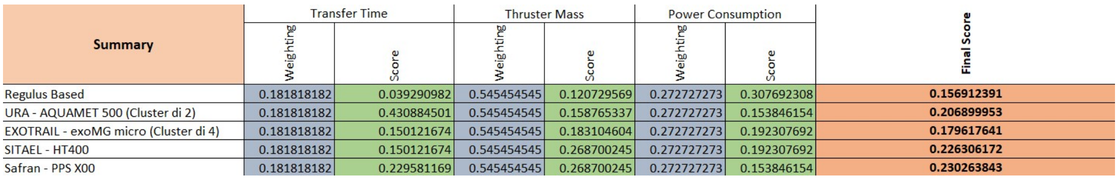

Summary	Transfer Time		Thruster Mass		Power Consumption		Final Score
	Weighting	Score	Weighting	Score	Weighting	Score	
Regulus Based	0.181818182	0.039290982	0.545454545	0.120729569	0.272727273	0.307692308	**0.156912391**
URA - AQUAMET 500 (Cluster di 2)	0.181818182	0.430884501	0.545454545	0.158765337	0.272727273	0.153846154	**0.206899953**
EXOTRAIL - exoMG micro (Cluster di 4)	0.181818182	0.150121674	0.545454545	0.183104604	0.272727273	0.192307692	**0.179617641**
SITAEL - HT400	0.181818182	0.150121674	0.545454545	0.268700245	0.272727273	0.192307692	**0.226306172**
Safran - PPS X00	0.181818182	0.229581169	0.545454545	0.268700245	0.272727273	0.153846154	**0.230263843**

Figure 4.18: Excel-table: trade-off results

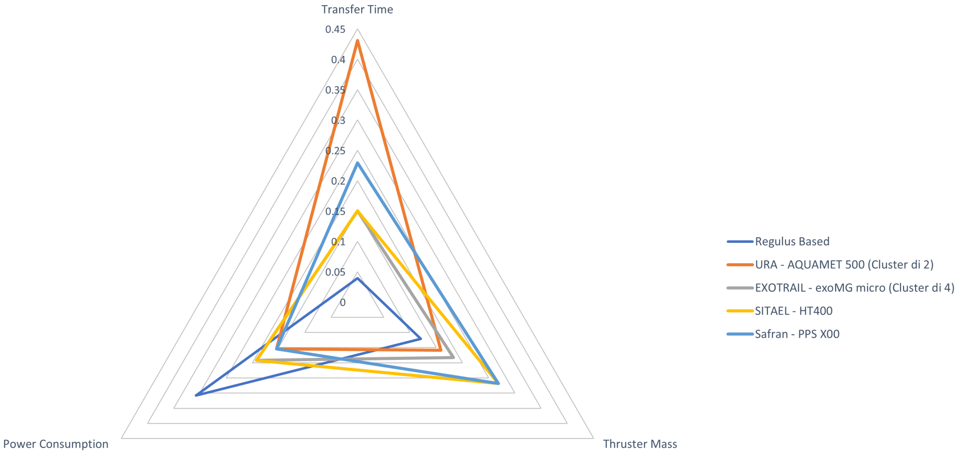

Figure 4.19: Radar graphic - Propulsion Trade-off

Chapter 5

Conclusions

On the basis of a widely spread analytical method for the mission analysis for spacecraft with electric propulsion, it has been identified, among the various proposals present in the market of electric thrusters, a solution as close as possible to the one that would be optimal to motorize a mission in LEO orbit dedicated to in-orbit servicing.

This first analysis, voluntarily and by the company's own choice, has been directed towards electric solutions only, and therefore Low-Thrust, which is certainly an important solution today, especially in the LEO-GEO environment; the analysis conducted here is therefore also appropriate for possible future developments of extension of the operational capabilities of IOSHEXA and can be considered in this perspective, an interesting starting point in the evaluation by SAB L.S., of the extension of the operational offer of the In-Orbit Servicing program that it is about to undertake.

Regarding the capability of IOSHEXA to act as a space-tug and therefore as a shuttle for cubesats and nano-satellites, it would be interesting, as in fact it is already the intention of the company, to consider a program that, in addition to an all-electric solution such as the one proposed in this work, would, above all for reasons of rapidity of response to customer needs, add more important thrust capabilities which, given the current technological levels, find their most immediate solution in the more classic chemical propulsion. A solution capable of combining the optimization possibilities of the electric and the readiness of the chemical would therefore be the most desirable at the moment.

Appendix A

ΔV Preliminary evaluation

```
clc;
clear all;
close all;
%%Constants and parameters:
% Earth Gravitational Constant [km^3/sec^2]:
mi = 398600;
% Earth Radius [km]:
Rp = 6371;
% Orbit Height Considered (Parking Orbit Height; Debris Orbit Height) [km]:
z = [550,823];
% Orbit inclinations [deg]:
incl = [97.59251383, 98.8];
% semi-major axis (orbit radius if circular orbit) [km]:
r = Rp+z;
% Total Specific Mechanical Energy of the considered Orbits [km^2/sec^2]:
Eg = -mi./(2*r);
Eg1 = Eg(1);
Eg2 = Eg(2);
% Circular Velocity [km/sec]:
v_c = sqrt(mi./r);
V_c1 = v_c(1);          %Circular velocity z = 550km
V_c2 = v_c(2);          %Circular velocity z = 823km
%%Impulsive Maneuvers:
%%Hohmann
i = 1;
% Periaps raising=> Hohmann transfer start
    v_h1 = V_c1*sqrt(2*r(2)/(r(1)+r(2)));
% Circularization
    v_h2= V_c2*sqrt(2*r(1)/(r(1)+r(2)));
```

```
% DeltaV [km/sec]
    DV1 = v_h1(1)-V_c1;
    DV2 = V_c2-v_h2(1);
% Total DeltaV [m/sec]
% DVTot (for transfer from 550 km to 823 km) [m/sec];
DVTot_hoh = (abs(DV2)+abs(DV1))*1e3
% Time Of Flight Hohmann Transfer:
T_Hohmann= pi*sqrt(((r(1)+r(2))/2)^3/mi);    %[sec]
T_Hohmann_Hours = T_Hohmann./(60*60)         %[hours]
%Simple Plane Change:
%Simple plane change is assumed, (conservative assumption) carried out at the %nodes and once at the elevation at which the debris to be collected is located.
% DV cambio di piano semplice [m/sec]
DV_simpl = 2*v_c(2)*sind((incl(2)-incl(1))/2)*1000
Cambio di piano e di inclinazione:
Delta_i = deg2rad(incl(2)-incl(1))      %[rad]
DV_combined = sqrt((V_c1^2)+(V_c2^2)-2*V_c1*V_c2*cos(Delta_i))*1000      %[m/sec]
%%Phasing
Assuming a 90 deg phasing in 1 day, assuming a phasing in more days the required DeltaVs are reduced. We perform the maneuver once we reach the altitude at which the debri orbits (z=823 km)
% Phasing Angle [deg]:
Angle = 90;
% Days available:
Days = 1;
Drift_rate = Angle/((Days*24*60*60)/(2*pi*sqrt(r(2)^3/mi)))
% DV required for phasing [m/sec]:
DV_phasing(i) = 2*Drift_rate*v_c(2)*1000/540        % 1080 o 540?
DV_walking = 2/3*(r(2)*pi)/((24*60*60))*1000        % MIT Lectures
%%Delayed Deorbit
%I assume in this case to lower the satellite to an altitude of 300 km so that %the aerodynamic actions of the atmosphere can then intervene causing the %satellite to decay.

% Deorbit Height [km]
H_deorbit = 300;
% DV [m/sec] (ref: SMAD pag 232) "The DeltaV requird for a satellite to drop from an initial circular
% altitude Hi to a reentry perigee altitude He is given by":
 DV_deorb_impulsive = v_c(2)*(1-sqrt(2*(Rp+H_deorbit)/(2*Rp+H_deorbit+z(2))))*1000
Total DeltaV (Impulsive)
 DV_total_Impulsive_Separated =(DVTot_hoh+DV_simpl+DV_phasing+DV_deorb_impulsive)
 DV_total_Impulsive =(DV_combined+DV_phasing+DV_deorb_impulsive)

```

```
%ESA Margins (Impulsive)
 DV_total_Impulsive_Separated_Margin = DV_total_Impulsive_Separated*(1+0.05)
 DV_total_Impulsive_Margin = DV_total_Impulsive*(1+0.05)

Low-Thrust Maneuvers
 Spiral Transfer
% DeltaV spiral [m/sec]:
     DV_spiral = abs(V_c1-V_c2)*1000
 Simple Plane Change Low Thrust:
 for i = 1:length(v_c)
     Di = incl(2)-incl(1);
     Di = deg2rad(Di);
     DV_simpl_LowThrust(i) = v_c(i)*sqrt(2-2*cos(pi*Di/2))*1000;
 end
DV_simpl_type1LT1 = DV_simpl_LowThrust(1)
DV_simpl_type1LT2 = D_simpl_LowThrust(2)
DV_simpl_LowThrust2 = Di*pi*v_c/2*1000; %Space Flight Dynamics
DV_simpl_type2LT1 = DV_simpl_LowThrust2(1)
DV_simpl_type2LT2 = DV_simpl_LowThrust2(2)
Combined Maneuvers:
DV_combined_LowThrust = sqrt(V_c1^2+V_c2^2-2*V_c1*V_c2*cos(Di*pi/2))*1000
 Walking:
DV_walking = 4/3*(r(2)*pi)/((24*60*60))*1000          % Worst case
 Delayed Deorbit Electric Propulsion
% I assume in this case to lower the satellite to an altitude of 300 km so that the aerodynamic actions of the atmosphere can then intervene causing the satellite to decay.
% Delayed Deorbit orbit radius  [km]
 r_deorbit = Rp+H_deorbit;
% Circular velocity deorbit orbit [km/sec]
 v_c_deorb = sqrt(mi/r_deorbit);
 DV_deorb_electric = abs(v_c_deorb-V_c2)*1000          %[m/sec]
% Total DV Low-Thrust:
DV_Total_LowThrust_Sep_Miss1 = DV_spiral+DV_simpl_type1LT1+DV_walking+DV_deorb_electric
DV_Total_LowThrust_Sep_Miss2 = DV_spiral+DV_simpl_type1LT2+DV_walking+DV_deorb_electric
DV_Total_LowThrust_Combined = DV_combined_LowThrust + DV_walking+DV_deorb_electric
% ESA Margins (L-T):
DV_Total_LowThrust_Sep_Miss1_margin = DV_Total_LowThrust_Sep_Miss1*(1+0.1)
DV_Total_LowThrust_Sep_Miss2_margin = DV_Total_LowThrust_Sep_Miss2*(1+0.1)
DV_Total_LowThrust_Combined_margin = DV_Total_LowThrust_Combined*(1+0.1)
```

Appendix B

Thrusting time

To evaluate the transfer time, we considered the thrusting time which, in the case of electric propulsion, can be assumed in good approximation to be coincident.

```
clc;
clear all;
close all;
%% Thruster parameters
% Input:
g0 = 9.81;
% Specific Impulses [sec] (Sequence: Regulus, AQUAMET, exoMG micro, HT400, PPS X00)
Isp = [500,800,1000,1529,1650];
% Initial Mass [kg]
m0 = 700;
% Delta v to be provided [m/sec]
Dv = 1015.5;
% Effective Exhaust Velocity [m/sec]
c = Isp*9.81;
% Thrust [N] (Sequence: Regulus, AQUAMET, exoMG micro, HT400, PPS X00)
T = [5,200,40,40,75]*10^-3
% Using the Rocket Equation and its results we have:
mp=m0*(1-exp(-Dv./c))
% Thrusting Time [sec]:
tb1 =((m0*c)./T).*(1-exp(-Dv./c))
% Thrusting Time [days]:
tb1_D = tb1/(60*60*24)
% Thrusting Time [yrs]:
tb1_Y = tb1_D/365
% Total Impulses:
I_tot = T.*tb1
```

Appendix C

Mission analysis for electric propulsion

C.1 Mission-Strategy-Technological Level

```
clc;
clear all;
close all
% Input:
 % [kW] Electric Power
% P_e = 2;
% [kg] Initial Mass
m_0 = 700;
% [m/sec^2] Gravitational acceleration
g0 = 9.81;
% [sec] Specific Impulses Vector
Isp = linspace (0,10000,1000);
% [m/sec] Effective Exhaust Velocity Vector
c = Isp*g0;
% Mission: DV is assigned [m/s]
DV = input("Enter the DV in [m/s] of the mission to be performed: ")
% Strategy: you define how much thrust [N] you have available
T = input("Enter a number between 0.5 and 500 to define the mN of thrust: ")*10^(-3)
% Technology: indicates the level of propulsion technology available [kg/W]
Beta = input("Define the Beta [kg/kW] technology level of the mission to be accomplished (typical range of values 1-50): ")*10^-3
% [kg] Final Mass
m_f_c = m_0*exp(-DV./c);
% [kg] Power Source Mass
```

```
m_s_c = m_0*Beta*T.*c/(2*m_0);
% [kg] Propellant Mass
m_p_c = m_0*(1-exp(-DV./c));
% [kg] Payload Mass m_u/m_0=1-(m_p/m_0)-(m_s/m_0)
m_u_c = m_0*exp(-DV./c)-m_0*Beta*T.*c/(2*m_0);
% Rating c of optimum
 c_ciclo = DV;
 err = 1;
 while err > 10^(-6)
     c_new = sqrt((2*m_0*DV*exp(-DV./c_ciclo))./(Beta*T));
     err = abs(c_new - c_ciclo);
     c_ciclo = c_new;
 end
M_f = m_f_c/m_0;
M_s = m_s_c/m_0;
M_p = m_p_c/m_0;
M_u = m_u_c/m_0;
C = c/DV
 plot(C, M_s,"LineWidth",1.5)
 hold on
 plot (C, M_f,"LineWidth",1.5)
 plot (C, M_p,"LineWidth",1.5)
 plot (C, M_u,"LineWidth",1.5)
 plot (c_new/DV*ones(1000,1),linspace(0,1,1000), "--","LineWidth",2,"Color",'b')
 plot (500*g0/DV*ones(1000,1),linspace(0,1,1000), "--","LineWidth",1,"Color",'y')
 plot (800*g0/DV*ones(1000,1),linspace(0,1,1000), "--","LineWidth",1,"Color",'m')
 plot (1000*g0/DV*ones(1000,1),linspace(0,1,1000), "--","LineWidth",1,"Color",'g')
 plot (1529*g0/DV*ones(1000,1),linspace(0,1,1000), "--","LineWidth",1,"Color",'c')
 plot (1650*g0/DV*ones(1000,1),linspace(0,1,1000), "--","LineWidth",1,"Color",'r')
 legend ("m_s/m_0","m_f/m_0","m_p/m_0","m_u/m_0","c_{opt}","REGULUS","AQUAMET","exoMG micro","HT400","PPS X00")
 ylabel ("m/m_0")
 xlabel ("c/\DeltaV")
 axis([0,100,0,1])
 Isp_ottimo = c_new/g0
% [kg] Final Mass with optimal Isp
m_f_c_opt = m_0*exp(-DV/c_new)
% [kg] Power Source Mass with optimal Isp:
m_s_c_opt = m_0*Beta*T*c_new/(2*m_0)
% [kg] Propellant Mass with optimal Isp:
m_p_c_opt = m_0*(1-exp(-DV/c_new))
% [kg] Payload Mass with optimal Isp:
m_u_c_opt = m_0*exp(-DV/c_new)-m_0*Beta*T*c_new/(2*m_0)
```

```
% Mission Duration [days]:
Tempo_MissioneDay = (m_p_c_opt*c_new/T)/(60*60*24)
% Thrust Power [W]:
T_power = T*c_new/2
```

C.2 Mission-Time-Technological Level

```
clc;
clear all;
close all
% Input:
 % [kW] Electric Power
% P_e = 2;
% [kg] Initial Mass
m_0 = 700;
% [m/sec^2] Gravitational acceleration
g0 = 9.81;
% [sec] Specific Impulses Vector
Isp = linspace (0,10000,1000);
% [m/sec] Effective Exhaust Velocity Vector
c = Isp*g0;
% Mission: DV is assigned [m/s]
DV_time = input("Enter the DV_time in [m/s] of the mission to be performed: ")
% Mission time: you define how long it takes to complete the mission:
Dt_time = input("Enter the number of days in which you want to complete the mission: ")*(60*60*24)
% Technology: indicates the level of propulsion technology available [kg/W]
Beta_time= input("Define the Beta [kg/kW] technology level of the mission to be accomplished (typical range of values 1-50): ")*10^-3
% [kg] Massa finale
m_f_DT = m_0*exp(-DV_time./c);
% [kg] Massa di propellente
m_p_DT = m_0*(1-exp(-DV_time./c));
% [kg] Massa del generatore
m_s_DT = m_0*Beta_time*c.^(2).*(m_p_DT/m_0)/(2*Dt_time);
% [kg] Massa di carico utile m_u/m_0=1-(m_p/m_0)-(m_s/m_0)
m_u_DT = m_0*exp(-DV_time./c)-m_0*Beta_time*c.^(2).*(m_p_DT./m_0)/(2*Dt_time);
c_ciclo_time = DV_time;
err = 1;
i = 1
while err > 10^(-6)
```

```
    c_new2 = Dt_time*exp(-DV_time/c_ciclo_time)/Beta_time*...
        ((DV_time/c_ciclo_time^2)+(Beta_time*DV_time/(2*Dt_time))+...
        (Beta_time*c_ciclo_time/Dt_time));
    err = abs(c_new2 - c_ciclo_time);
    c_ciclo_time = c_new2;
    i = i + 1;
end
M_f_time = m_f_DT/m_0;
M_s_time = m_s_DT/m_0;
M_p_time = m_p_DT/m_0;
M_u_time = m_u_DT/m_0;
C_time = c/DV_time
plot(C_time, M_s_time,"LineWidth",1.5)
hold on
plot (C_time, M_f_time,"LineWidth",1.5)
plot (C_time, M_p_time,"LineWidth",1.5)
plot (C_time, M_u_time,"LineWidth",1.5)
plot (c_new2/DV_time*ones(1000,1),linspace(0,1,1000), "--","LineWidth",2,"Color","b1")
plot (500*g0/DV_time*ones(1000,1),linspace(0,1,1000), "--","LineWidth",1,"Color",'y')
plot (800*g0/DV_time*ones(1000,1),linspace(0,1,1000), "--","LineWidth",1,"Color",'m')
plot (1000*g0/DV_time*ones(1000,1),linspace(0,1,1000), "--","LineWidth",1,"Color",'g')
plot (1529*g0/DV_time*ones(1000,1),linspace(0,1,1000), "--","LineWidth",1,"Color",'c')
plot (1650*g0/DV_time*ones(1000,1),linspace(0,1,1000), "--","LineWidth",1,"Color",'r')
legend ("m_s/m_0","m_f/m_0","m_p/m_0","m_u/m_0","c_{opt}","REGULUS","AQUAMET","exoMG micro","HT400","PPS X00")
ylabel ("m/m_0")
xlabel ("c/\DeltaV")
axis([0,100,0,1])

C_DV = c_new2/DV_time
c_ciclo_time = DV_time;
err = 1;
i = 1
while err > 10^(-6)
    c_new2 = Dt_time*exp(-DV_time/c_ciclo_time)/Beta_time*...
        ((DV_time/c_ciclo_time^2)+(Beta_time*DV_time/(2*Dt_time))+...
        (Beta_time*c_ciclo_time/Dt_time));
    err = abs(c_new2 - c_ciclo_time);
    c_ciclo_time = c_new2;
    i = i + 1;
end
M_f_time = m_f_DT/m_0;
M_s_time = m_s_DT/m_0;
```

```
M_p_time = m_p_DT/m_0;
M_u_time = m_u_DT/m_0;
C_time = c/DV_time
plot(C_time, M_s_time,"LineWidth",1.5)
hold on
plot (C_time, M_f_time,"LineWidth",1.5)
plot (C_time, M_p_time,"LineWidth",1.5)
plot (C_time, M_u_time,"LineWidth",1.5)
plot (c_new2/DV_time*ones(1000,1),linspace(0,1,1000), "--","LineWidth",2,"Color","b1")
plot (500*g0/DV_time*ones(1000,1),linspace(0,1,1000), "--","LineWidth",1,"Color",'y')
plot (800*g0/DV_time*ones(1000,1),linspace(0,1,1000), "--","LineWidth",1,"Color",'m')
plot (1000*g0/DV_time*ones(1000,1),linspace(0,1,1000), "--","LineWidth",1,"Color",'g')
plot (1529*g0/DV_time*ones(1000,1),linspace(0,1,1000), "--","LineWidth",1,"Color",'c')
plot (1650*g0/DV_time*ones(1000,1),linspace(0,1,1000), "--","LineWidth",1,"Color",'r')
legend ("m_s/m_0","m_f/m_0","m_p/m_0","m_u/m_0","c_{opt}","REGULUS","AQUAMET","exoMG micro","HT400","PPS X00")
ylabel ("m/m_0")
xlabel ("c/\DeltaV")
axis([0,100,0,1])
C_DV = c_new2/DV_time
% Optimal specific pulse assigned days:
Isp_ottimo = c_new2/g0
% [kg] Final Mass with optimal Isp
m_f_DT_opt = m_0*exp(-DV_time./c_new2)
% [kg] Propellant Mass with optimal Isp:
m_p_DT_opt = m_0*(1-exp(-DV_time./c_new2))
% [kg] Power Source Mass with optimal Isp:
m_s_DT_opt = m_0*Beta_time*c_new2.^(2).*(m_p_DT_opt/m_0)/(2*Dt_time)
% [kg] Propellant Mass with optimal Isp:
m_u_DT_opt = m_0*exp(-DV_time./c_new2)-m_0*Beta_time*c_new2.^(2).*(m_p_DT_opt./m_0)/(2*Dt_time)
% [N] Thrust to be provided
T_time = m_p_DT_opt/Dt_time*c_new2
% [mN] Thrust to be provided in milliNewton
T_time_mN = m_p_DT_opt/Dt_time*c_new2*10^3
% [kW] Thrust Power
T_power_time = T_time*c_new2/2*(10^(-3))
```

Bibliography

[1] Matteo Tugnoli, Martin Sarret, and Marco Aliberti. *European Access to Space: Business and Policy Perspectives on Micro Launchers.* Springer, 2019 (cit. on p. 1).

[2] Heiner Klinkrad. «Space debris». In: *Encyclopedia of Aerospace Engineering* (2010) (cit. on p. 5).

[3] «Active Debris Removal- ESA». In: (). URL: `http://www.esa.int/Safety_Security/Space_Debris/Active_debris_removal` (cit. on p. 7).

[4] Jerry E. White Roger R. Bate Donald D. Mueller. *Fundamentals of Astrodynamics.* Dover Pubblications, 1971 (cit. on p. 11).

[5] Jason R. Wertz Wiley J. Larson. *Space Mission And Design.* Space Technology Library, 1992 (cit. on pp. 18, 20, 26).

[6] Mirko Leomanni, Gianni Bianchini, Andrea Garulli, and Antonio Giannitrapani. «A class of globally stabilizing feedback controllers for the orbital rendezvous problem». In: *International Journal of Robust and Nonlinear Control* 27 (Dec. 2017), pp. 4296–4311. DOI: `10.1002/rnc.3817` (cit. on p. 18).

[7] Craig A Kluever. *Space flight dynamics.* John Wiley & Sons, 2018 (cit. on pp. 20, 21, 23, 25, 26, 29, 33, 35, 38, 39).

[8] Casalino L. *Space Propulsion.* 2020 (cit. on pp. 24, 32, 34, 53).

[9] Armando Ruggiero, Pierpaolo Pergola, Salvo Marcuccio, and Mariano Andrenucci. «Low-thrust maneuvers for the efficient correction of orbital elements». In: *32nd International Electric Propulsion Conference.* 2011, pp. 11–15 (cit. on pp. 38, 39).

[10] Gunnar Tibert. *Fundamentals of Spaceflight.* 2019 (cit. on p. 39).

[11] Manuel Martinez-Sanchez and Paulo Lozano. *MIT OpenCourseWare: 16.522 Space Propulsion, lecture 6.* 2015 (cit. on pp. 40, 41).

[12] Manuel Martinez-Sanchez and Paulo Lozano. *MIT OpenCourseWare: 16.522 Space Propulsion, lecture 16.* 2015 (cit. on pp. 44, 45).

[13] M Manente, F Trezzolani, M Magarotto, E Fantino, A Selmo, N Bellomo, E Toson, and D Pavarin. «REGULUS: A propulsion platform to boost small satellite missions». In: *Acta Astronautica* 157 (2019), pp. 241–249 (cit. on pp. 46, 47, 63).

[14] J.E. Brandenburg, J. Kline, and D. Sullivan. «The microwave electro-thermal (MET) thruster using water vapor propellant». In: *IEEE Transactions on Plasma Science* 33.2 (2005), pp. 776–782. DOI: `10.1109/TPS.2005.845252` (cit. on p. 48).

[15] «Hall Effect Thrusters - Advanced Propulsion - Sitael». In: (). URL: `https://www.sitael.com/space/advanced-propulsion/electric-propulsion/hall-effect-thrusters/` (cit. on p. 62).

[16] «Safran, a major player in plasma propulsion». In: (). URL: `https://www.safran-group.com/media/safran-major-player-plasma-propulsion-20180605` (cit. on p. 62).

[17] «Exotrail-Hall Effect Thrusters for small satellite». In: (). URL: `https://exotrail.com/product/` (cit. on p. 62).

[18] «REGULUS Electric Propulsion System». In: (). URL: `https://www.t4innovation.com/regulus-electric-propulsion-system/` (cit. on p. 63).

[19] «AQUAMET Electric Propulsion System». In: (). URL: `https://www.urathrusters.com/` (cit. on p. 63).

[20] Daniela Pedrini, Cosimo Ducci, Tommaso Misuri, Fabrizio Paganucci, and Mariano Andrenucci. «Sitael hollow cathodes for low-power Hall effect thrusters». In: *IEEE Transactions on Plasma Science* 46.2 (2017), pp. 296–303 (cit. on p. 64).

[21] J Vaudolon, V Vial, N Cornu, and I Habbassi. «PPS R@ X00 Thruster Development Status at Safran». In: (2019) (cit. on p. 64).

Ringraziamenti

A conclusione di questo lavoro di tesi è mia premura ringraziare quanti, con i loro suggerimenti e le loro conoscenze, hanno contribuito alla sua riuscita.
Il primo ringraziamento va certamente alla mia relatrice, la professoressa Battipede, e al mio correlatore, ingegner Mascolo, che mi hanno dato l'opportunità di approfondire e fare mie, in collaborazione con la SAB Launch Services srl, argomenti e tematiche di estremo interesse.
Un ulteriore grazie va poi rivolto all'azienda ed in particolare al dottor Fragnito che mi ha sempre seguito con estrema disponibilità, consentendomi di scambiare idee e collaborare con varie ed importanti aziende spaziali europee.